Characterizing ecoregions based on the chemical characteristics of lake sediments

Bowen Xiao

Thesis submitted to the University of Ottawa
in partial Fulfillment of the requirements for the
MSc

Department of Biology
Faculty of Science
University of Ottawa

Abstract

Earth's climate is prone to natural and episodic cycles. The most recent period of climate change, the only one to be caused by humans, is significantly affecting species composition and landscapes. Northern expansion of the Boreal Forest in Canada is one of the expected outcomes, and tree line migration northward is one of the anticipated changes. Previous studies have found that many human activities like agriculture, grazing, and pastoralism can significantly affect tree line movement. Improving our ability to examine past tree line dynamics can be achieved using archival records in lake sediments. In this study, we focused on three sediment biomarkers that may be related to the presence of trees in a lake's catchment: *n*-alkanes, lignin-derived phenols, and stable isotopes of carbon. We examined the composition of these markers in sediment from 19 lakes in Saskatchewan spanning 4 ecoregions, from Prairie Grassland to Boreal Plain, to determine the biomarker signature for lakes in each ecoregion and relating them to land cover (trees vs herbaceous plants) in the catchments of each lake. The results showed that *n*-alkane composition was significantly correlated to the proportion of trees to herbaceous plants in a lake's catchment, raising the possibility that these can be used to infer the presence of trees in sediment records. The C/N ratio and $\delta^{13}C$ were not effective in distinguishing ecoregions or land cover composition, likely due to algal production in the lake and agricultural activities in the surrounding farmland, while lignin-derived phenols appeared to be affected by unknown factors.

Keywords: *n*-alkanes, lignin-derived phenols, stable isotopes, lake trophic status, lake sediments, tree line

Acknowledgments

Thank you so much Dr. Jules Blais for providing me with a great chance to join your lab and work on this project. Thank you to Dave Eickmeyer and Linda Kimpe for all your guidance on the lab work and background knowledge. Your patience in replying to all my emails and your understanding of my difficulties have supported me through the past two years. These mean a lot to me, and the work would not have been done without you. Thank you to our team members Milla Rautio, Henriikka Kivilae, and Vilmantas Preskienis in Milla's laboratory at UQAC for your help on the field works and trophic status analysis. Thank you to Myrna J. Simpson and Meiling Man in Simpson laboratory at the University of Toronto in Scarborough for helping me with lignin-derived phenols analysis and for replies to my questions. Thank you to everyone in Jan Veizer Stable Isotope Laboratory at the University of Ottawa for helping me with the stable isotope analysis. Thank you to Hugo Crites in the Geographic, Statistical and Government Information Centre (GSG) at the University of Ottawa for technical and methodological support on ArcGIS. Thank you to Dene Cheecham-Uhrich and Paul Haynes in Clearwater River Dënë School in Saskatchewan for your support and guidance during the field work. Lastly, thank you to everyone in the Blais lab, it's my pleasure to work with a group of intelligent and enthusiastic people like you.

Table of Contents

List of Figures

List of Tables

Chapter 1 Introduction

Recent climate change is a major challenge facing modern society, but the Earth's climate is prone to natural and episodic cycles. Recent climate change must therefore be examined in the context of long-term climate variability. For example, over the scale of hundreds of thousands of years, Earth's climate has fluctuated between glacial and interglacial cycles, likely due to the cyclicity of the Earth's orbit (Ruddiman, 2000), during which time air temperatures and CO_2 concentration in the atmosphere have varied in tandem (e.g. Lüthi et al. 2008). In recent decades, global temperatures and atmospheric CO_2 have drastically increased because of human activities (MacDonald, 2010; US Department of Commerce, 2022). A summary from the Intergovernmental Panel on Climate Change (IPCC 2021) reported that the global average temperature from 2011-2020 had increased by 1.09 °C since 1850-1900 (Masson-Delmotte et al., 2021), and the World Meteorological Organization (WMO) similarly reported 1.2 °C warming in 2020 above the pre-industrial era (*State of the Global Climate 2020*, 2021). In contrast, little net warming was observed between the 18th and 19th Centuries, and recent warming greatly exceeds natural variation estimates. This recent increase in temperature has caused impacts on populations, ecosystems, and landscapes over the past hundred years.

Prior to the Industrial Age, temperature anomalies including the Medieval Warm Period (MWP, 950 AD – 1250 AD) the Little Ice Age (LIA, 1500 AD – 1700 AD), and the Roman Warm Period (250 BC-400 AD) are evidence that climate variability has

occurred at other times in history (Adhikari & Kumon, 2001; Carlson, 1977; Cronin et al., 2003; Lamb, 1965; Lécuyer et al., 2021; Yamada et al., 2010). These more recent climatic anomalies have been attributed to multiple factors, including variations in solar activity (Parker, 1999), volcanic activity (Aubry et al., 2022; Bryson & Goodman, 1980), and changes to oceanic circulation patterns (Bianchi & McCave, 1999). Thus, recent climate change must be examined in the context of these other cyclical and episodic variabilities.

Recent climate warming has had profound impacts on global ecosystems. For example, Leemans & Eickhout (2004) used the IMAGE model to implement IPCC-SRES scenarios to study the impacts of human activities on ecosystems, and they found changes in temperature consistent with climate warming scenarios (1°C~2°C) can significantly affect species composition and landscapes. In northern areas like Canada, one of the expected outcomes of climate warming is the northern expansion of the Boreal Forest toward the tundra region (ACIA, 2005).

The tree line refers to the edge of the forest, where the environmental conditions beyond the tree line do not support the growth of trees (Körner & Paulsen, 2004). Previous studies showed that the tree line is very sensitive to the impact of global temperature change (Bharti et al., 2012; Gaire et al., 2017; Mishra & Mainali, 2017; Weisberg et al., 2018). The projected increase in temperatures could cause the northward expansion of the Boreal Forest, which may also influence the forest's

ability to sequester carbon (ACIA, 2005). Thus, it is meaningful and important to develop a method to track and estimate tree line migration over long-time scales (centuries-millennia).

Several factors have been shown to contribute to tree line shifts. For example, Gehrig-Fasel et al. (2007) studied the tree line shift in Switzerland between 1985 to 1997 and found that the forest grew back quickly to reduced alpine farming, reduced agriculture, and less intensive grazing. Cudlín et al. (2017) and other studies reported that land use affected tree line in different European mountains, as the alpine grassland was lost to uncontrolled grazing while burning and pastoral activities modified the species' distribution in the Alp (Theurillat & Guisan, 2001) s. Naccarella et al. (2020) studied the tree line shift in the Victorian Alps and found that fire can strongly impact tree line dynamics. Wotton et al., (2017) evaluated the effect of climate change on potential crown fire occurrence and activity fire growth and reported that "the proportion of days in fire seasons with the potential for unmanageable fire will increase across Canada's forest", which was realized in 2023 when over 150000 km^2 of forest was burned in Canada alone (*CIFFC | Fire Statistics*, 2023). Thébault et al. (2014) suggested that soil microbial communities (fungal-dominated communities) compete with trees for inorganic N through N immobilization, which could eventually limit tree line expansion in high latitudes. Given that there are so many factors that can affect tree line, improving our ability to project future tree line will have far-reaching implications for the role of Canada's

Boreal Forest, as a major carbon sink, in the global carbon balance.

To better predict the future of northern ecosystems, it is informative to see how and whether tree lines migrated in the past. Some methods to study tree line movements include dendrochronology and measurement of tree diameter, but these studies are limited to short time scales (Prabinarana et al., 2017; Schweingruber, 2012). Dendrochronology can only reveal changes in the past few decades or at most centuries, whereas past changes in tree line relative to climate change have a much longer history. Comparatively, Viau & Gajewski (2009) tracked tree line positions from lake sediment cores using biogenic proxies such as pollen, macrofossils, charcoal, and diatoms. Although much information can be garnered from these approaches, they are limited due to varying levels of proxy sensitivity. For example, pollen can travel by air over hundreds of kilometers, challenging its use as a tree line marker.

A longer perspective on past tree line dynamics can help inform predictions of future tree line dynamics. Paleolimnology is the study of lake sediment records that can often extend records back to the early Holocene or earlier. These studies focus on reconstructing the ecological history of inland waters (streams, lakes, and watersheds) using pollen records, diatoms, organic matter characterization, and other indicators from dated lake sediment deposits. These records can provide information on climate change, eutrophication, acidification, and other environmental changes. As the

environment changes, biological products in sediments, including organic molecules, can help us track those changes. Those biomarkers that flow into lakes quickly deposit on the bottom and become part of the lake sediment record. We may then collect the lake sediment cores and observe the biomarkers and how they changed over time to reconstruct the environment around the lake. Depending on the lakes in different ecoregions, we can reconstruct environmental and ecological history with a timeline of hundreds to thousands of years in the past.

The objective of this study was to identify sediment biomarkers that may be useful to characterize sediments from the different ecotones in Saskatchewan. Ecotones are the steep transition areas between distinct ecosystems with different ecological features, like Prairie Grassland to Aspen Parkland (Riser, 1990). We focused our sampling on Saskatchewan (Canada), which has a complex ecological composition, spanning from Prairie Grassland, Aspen Parkland, Boreal Transition, and Boreal Plain Upland, including the southern tree line spanning between Prairie Grassland and Aspen Parkland. In total, we sampled sediments from 19 lakes from the following ecoregions in Saskatchewan: Prairie Grasslands, Aspen Parkland, Boreal Transition, and Boreal Uplands (Fig. 1.1).

Fig. 1.1. Sampled lakes and the ecoregions in Saskatchewan. Tree line is indicated in red.

The Boreal Upland is bordered in the north by the Boreal Plain and Boreal Shield

transition, and in the south by the Boreal Transition ecoregion. It is a mix of coniferous trees (woody gymnosperms) like Pinaceae and Cupressaceae, and aspens (woody angiosperms) like trembling aspen (*Populus* spp.) (Brandt et al., 2013; Herbarium, 2008). The Boreal Transition ecoregion is at the southern end of the Boreal Plain ecozone. The dominant species are conifers and aspens, but conifers in Boreal Transition are less common than Boreal Upland (Herbarium, 2008). Aspen Parkland is the northern end of the Prairie ecozone, which is dominated by aspen, oak groves, mixed tall shrubs, and intermittent fescue (C3) grasslands (Herbarium, 2008). The Prairie Grassland is part of the temperate grasslands, savannas, and shrublands biome, dominated by spear grass and wheat grass (graminoids), and deciduous shrubs (woody angiosperms) (Herbarium, 2008). The variety of woody plants and grass should affect the chemical composition of sediments, which may be useful for tracking changes in ecotones based on lake sediment records (Saleem et al., 2019).

Biomarkers are chemical indicators in organic matter. We can often determine the origin of organic matter based on the composition of biomarkers in lake sediment. Saleem et al. (2019) showed that many biomarkers like lignin-derived phenols and *n*-alkanes had been used effectively for historical reconstructions, yet not integrated into tree line reconstruction. Saleem et al. (2019) proposed a unique metabolomics-derived methodology for untargeted analysis of sediment biomarkers, which provided a means to determine how organic matter composition differs among ecoregions, especially for studies of tree line.

Here I develop some targeted methods to determine the utility of chemical markers in sediment, including stable isotopes ($\delta^{13}C$), leaf epicuticular waxes (*n*-alkanes), and lignin-derived phenols, to characterize lake sediment from specific ecoregions in Saskatchewan and the Northwest Territories, specifically for the purpose of determining relative contributions from trees and herbaceous plants to sediments. Given that sediments can be dated precisely by radiometric methods, these sediment biomarkers may therefore be useful for determining when changes in tree line position occurred in the past.

***n*-Alkanes:**

Leaf wax *n*-alkanes are long carbon chains of varying lengths (Fig. 1.2) produced as leaf epicuticular waxes and they function as a protection layer in leaves and needles (Post-Beittenmiller, 2003). All terrestrial, emergent, and submerged plants have these lipids to help retain water and/or provide leaf protection, but the composition of *n*-alkanes can change depending on the plants (Lockheart et al., 1997) and may also have a small variance within species through the growing seasons (Sachse et al., 2009). Furthermore, different environmental conditions (Sachse et al., 2010), species (Meyers, 2003), etc. can also affect the composition of *n*-alkanes (Lockheart et al., 1997).

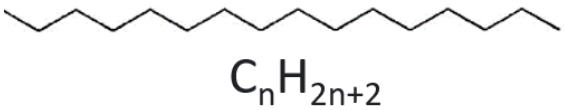

C_nH_{2n+2}

Fig. 1.2. An example of *n*-alkanes. The *n* refers to the 'normal' (i.e. straight-chain) configuration in the molecule.

Due to the stability of the straight-chain hydrocarbons, *n*-alkanes can survive in a relatively stable sedimentary environment, even for millions of years (Eglinton & Logan, 1991). This project examines the composition of different *n*-alkanes in lake sediments from the different ecotones in Saskatchewan that have a wide range of dominant plant species in the catchments. *n*-Alkanes in plant waxes generally have a predominance of odd-number carbons (Cranwell, 1973; Eglinton & Hamilton, 1967; Otto, Simoneit, et al., 2005) because they are synthesized by decarboxylation of even-numbered fatty acids. According to dominant species in different ecozones (mosses, wooden plants, or grasses), variations of *n*-alkanes in different plant species and environmental conditions have been studied and used to trace the source and delivery processes of terrestrial organic matter (Seki et al., 2010). The C17 alkane is primarily produced by algae (Cranwell et al., 1987), whereas Ficken et al. (2000) found C23-C25 are mostly from non-emergent (aquatic) plants. Emergent (aquatic) plants were seen to have a similar *n*-alkane composition with terrestrial plants having *n*-alkanes >C29. Cranwell (1973) suggested that C27 and C29 may be more abundant in lake sediments where the watersheds are dominated by deciduous and coniferous trees, and C31 should be more abundant in sediments of lakes where the major input is from grasses, but they did not demonstrate this quantitatively. These studies do suggest that the composition of *n*-alkanes can provide information about the

predominant sources of organic matter, which may therefore allow us to distinguish sediments with different land covers in their catchments. Considering the lake sediment is a mixture of biomaterials from both woody and nonwoody plants from various sources, we decided to focus our study on the relationship between *n*-alkane composition and the proportion of terrestrial woody plants in the watershed of the studied lakes. We focused on C_{27}, C_{29}, and C_{31} which are the dominant *n*-alkanes of grasses and trees.

Lignin-derived phenols:

Lignin-derived phenols are classified into four basic classes, which are p-hydroxyl, vanillyl, syringyl, and cinnamyl phenols (Fig. 1.3). Compared with other sediment biomarkers, lignin-derived phenols could better present the differences between ecoregions on land because lignin is produced entirely by terrestrial organic matter (Hedges & Mann, 1979a). Given that lignins are not produced by aquatic plants, they effectively track the organic matter influx from land to lake sediments and may help us distinguish between the ecotones considered here (Hedges & Mann, 1979a).

Analyzing the concentration of lignin-derived phenols in the sediment can provide statistically meaningful results reflecting the woody plants present in an area, which can eventually be used to track long-term tree line movement in dated lake sediment cores. Moreover, Hedges & Mann, (1979b) plotted the lignin-derived phenols of different plants and showed that they produce distinctive types of phenols (Fig. 1.4).

Gymnosperm woods only contain vanillyl derivatives with low S/V and C/V ratios, while vanillyls and syringyls derivatives in angiosperms are about equal (Hedges & Mann, 1979a). Other than woody tissues, non-woody tissues in gymnosperms and angiosperms like leaves and grasses contains high cinnamyl derivatives (Iiyama et al., 1990; Lam et al., 2001). Thus, we can analyze the phenol types in the lake sediment and plot the S/V and C/V ratios to determine relative contributions from gymnosperms (conifers) and angiosperms (mainly deciduous trees). We predict that the samples from the Boreal Upland will contain a more even mix of gymnosperm and angiosperm woody sources, whereas Boreal Transition samples will contain more angiosperms, Aspen Parkland will be weighted more toward angiosperm woody sources, and Prairie grasslands will fall into angiosperm nonwoody space as shown in Fig. 1.4.

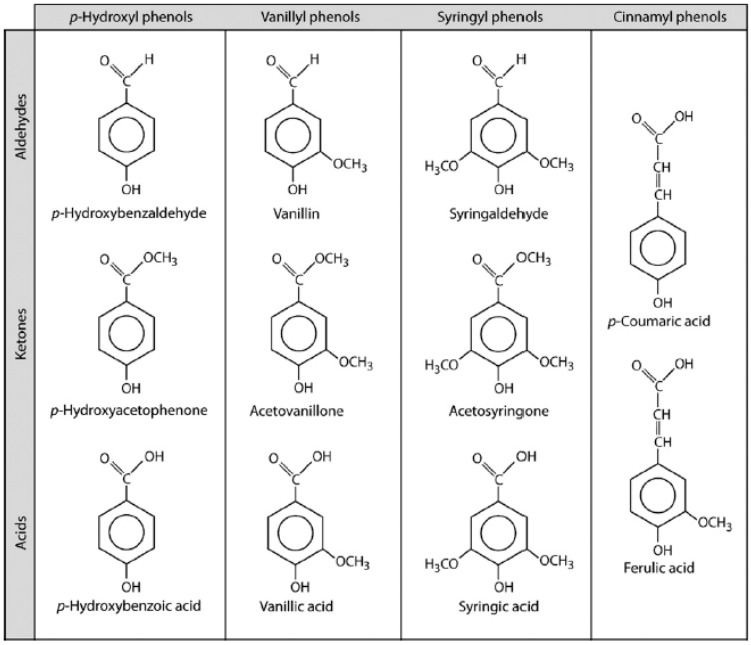

Fig. 1.3. Lignin-derived phenols with the alkaline CuO oxidation: H-type, V-type, S-type, and C-type phenols. Figure from Thevenot et al. (2010).

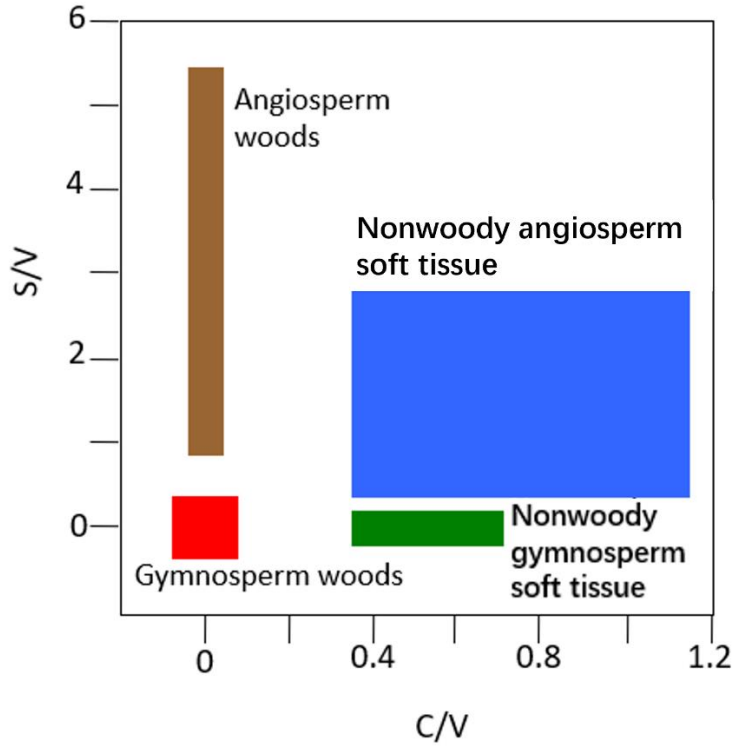

Fig. 1.4. Plots of lignin parameters for surface sediments. S/V: Syringyl/Vanillyl. C/V = Cinnamyl/Vanillyl. The plot was generated based on the results from (Hedges & Mann, 1979b).

Stable isotopes of carbon:

Stable isotopes are elements that do not decay into other elements or other isotopes over time. Their abundance in various environmental media has been useful to reveal different sources of organic matter (Meyers, 1997). When plants perform photosynthesis, they absorb and reduce inorganic carbon (CO_2) and release oxygen. The proportion of ^{13}C (1.1%) as CO_2 and CH_4 is much lower than ^{12}C (98.9%) (O'Leary, 1988), and the $^{13}C/^{12}C$ ratio is even lower in plants because photosynthesis tends to assimilate the lighter ^{12}C preferentially over the heavier ^{13}C. The different photosynthetic pathways used by C3 and C4 plants therefore result in different $\delta^{13}C$

values, providing information on the source of C.

The $\delta^{13}C$ of bulk organic C may also be used as a proxy to identify if the primary OM source is C3 or C4 plants. Differences between C3 and C4 plants on $\delta^{13}C$ and C/N ratios are in Fig. 1.5, where C3 plants (-33 to -24 ‰) have much lower $\delta^{13}C$ than C4 plants (−16 to −10‰, (O'Leary, 1988). C4 plants convert CO_2 into bicarbonate, then the enzyme phosphoenolpyruvate (PEP) carboxylase fixes it to oxaloacetate to produce malate (Hayes, 2001). Malate is then transported to the bundle sheath cells, re-oxidized, and decarboxylated back into CO_2 and pyruvate to maintain high internal CO_2 and avoid competing photorespiration reactions (Hayes, 2001). This process concentrates $^{13}CO_2$ and results in higher $\delta^{13}C$ values in C4 plants (such as grasses in the studied ecoregions). In this study, we will determine $\delta^{13}C$ in bulk sediments using Equation 1:

Equation 1.
$$\delta^{13}\mathrm{C} = \left(\frac{\left(\frac{^{13}\mathrm{C}}{^{12}\mathrm{C}}\right)_{\mathrm{sample}}}{\left(\frac{^{13}\mathrm{C}}{^{12}\mathrm{C}}\right)_{\mathrm{standard}}} - 1 \right) \times 1000$$

$\delta^{13}C$ can therefore help us identify whether C3 or C4 plants predominate as sources of organic matter in lakes and should in principle be higher in Prairie Grasslands lake sediments than in the forested Aspen Parklands, Boreal Plains, and Boreal Uplands.

Our goal is to determine a biomarker signature for sediments of lakes in the studied ecoregions using the results of the targeted biomarker analysis. If we can distinguish sediments in lakes from each of the different ecoregions, we hypothesize that the

composition of lake sediments in dated sediment cores may reveal details about changes in organic matter sources and therefore in land cover type over time in more detailed paleolimnological investigations.

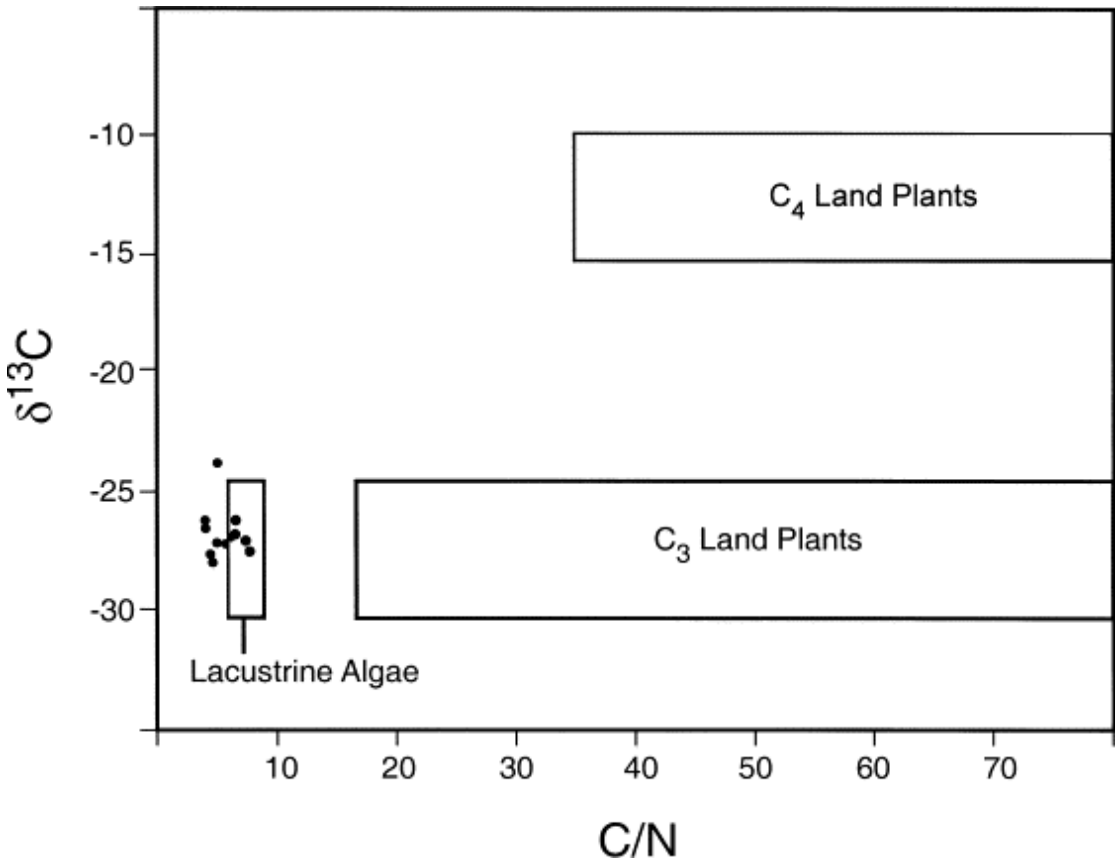

Fig. 1.5. Plotted $\delta^{13}C$ and C/N ratios of C3, C4, and algae in the lake sediment. Figure from Meyers (2003).

Chapter 2 Methods

2.1 Sample site selection

We sampled 19 lakes from the following 4 ecoregions in Saskatchewan (Canada): Prairie Grassland, Aspen Parkland, Boreal Transition, and Boreal Upland (from Southern and Northern end). For each ecoregion we have about an equal number of sampled lakes. The location and information of the lakes are summarized in Table 2.1. This selection spans a wide range of land cover, from grasslands with no trees to completely forested catchments. We selected only headwater lakes to minimize biomaterials transported from different ecoregions and to provide the clearest signals for the studied ecoregions. Similarly, we selected smaller lakes (ranging from 0.2-6.3 km^2) for consistency among sites, they had catchment area to lake area ratios that spanned from 1.6-126.3. Small lakes were also chosen to maximize OM contributions from catchments to sediments. To minimize the effect of human activities, we chose sites with low impact from residential and agricultural activities in lake catchments. For example, all lakes in the Prairie Grassland region of Saskatchewan were situated in parks, where agricultural impacts are minimized.

Table 2.1. Summary of the sampled lakes in Saskatchewan. Data collected from HydroLAKES database. Maxium depth measured with bathymetry (if available).

Lake	Lat	Long	Ecoregion	Lake area (km^2)	Catchment area (km^2)	Catchment:lake area	Mean Depth (m)	Maximum Depth (m)
Amber Lake	57°26'43.89"N	109°15'47.50"W	Mid-Boreal Plain Uplands	0.24	16.6	68.2	3.6	
Bray Lake	57°26'52.76"N	109°22'16.77"W	Mid-Boreal Plain Uplands	2.41	14.3	4.9	4.7	
Fontaine Lake	57°12'47.22"N	109°04'11.11"W	Mid-Boreal Plain Uplands	0.23	0.6	1.6	1.8	
Sinclair Lake	56°52'53.28"N	108°56'41.82"W	Mid-Boreal Plain Uplands	1.19	77.8	64.4	6.4	
Heritage Lake	53°55'47.03"N	105° 9'8.80"W	Mid-Boreal Plain Uplands	2.76	20.5	6.4	3.3	15.4
Jeannette Lake	54°32'11.58"N	108°32'38.63"W	Mid-Boreal Plain Uplands	3.83	13.1	2.4	6.2	33.3
McPhee Lake	53°52'33.00"N	105°57'48.95"W	Mid-Boreal Plain Uplands	1.88	38.1	19.3	5.8	7.3
Zeden Lake	53°59'17.89"N	104°40'20.73"W	Mid-Boreal Plain Uplands	0.3	1.1	2.7	2.8	
Eagle Lake	52°38'29.40"N	104°37'53.50"W	Boreal Transition	1.29	120.8	92.6	4.8	7
Jimmy (Pratt) Lake	53°14'32.62"N	106°52'19.83"W	Boreal Transition	1.29	63.1	33.3	5.4	17.4
Lac la Pêche	52°56'40.79"N	107° 4'15.89"W	Boreal Transition	0.99	47.2	46.7	5.4	11.9
Matheson Lake	54°24'34.29"N	108°56'20.97"W	Boreal Transition	3.29	42	11.8	4.5	17.7
Dillberry Lake	52°34'40.19"N	110° 0'19.42"W	Aspen Parklands	0.4	14.7	35.8	2.5	
Picnic Lake	53°12'26.17"N	108°39'41.19"W	Aspen Parklands	0.49	29.3	58.8	3.5	
Suffern Lake	52°38'15.16"N	109°53'55.21"W	Aspen Parklands	0.24	19.9	81.9	3.2	7.9
Twin Lakes	52°49'51.79"N	108°31'26.80"W	Aspen Parklands	0.64	18.1	27.3	4.4	
Antelope Lake	50°16'42.00"N	108°23'14.00"W	Prairie Grasslands	6.09	775.3	126.3	2.3	11.3
Clearwater Lake	50°52'23.54"N	107°55'43.14"W	Prairie Grasslands	0.56	7.3	12.0	3.4	10.1
Lac Pelletier	49°58'23.16"N	107°55'56.24"W	Prairie Grasslands	3	77.4	24.8	9.1	11.6

2.2 Sample collection

In August 2021 and 2022, we used a Uwitec gravity corer and polycarbonate core tubes to collect 4 sediment cores from the deepest part of each lake, or the deep and flat region of the lakes if the deepest site was undetectable. One core was sectioned into 1 cm intervals, and the other three were sectioned for top sediments (0 - 2 cm) and deep sediments (20 - 22 cm). Sediment samples were then stored in Whirl-Pak® bags, frozen, and transported to the laboratory at the University of Ottawa, then stored at -20 °C. Subsamples were freeze-dried for further analysis.

2.3 Sediment analyses

2.3.1 n-Alkane analysis

For each sampled lake, 0.5 g of dry sediment samples were mixed with the diatomaceous earth (rinsed with petroleum ether), packed in the accelerated solvent extractor (ASE) cells and extracted by ASE (at 100 °C, 1450 psi) with 9:1 DCM: MeOH (21 ml for each sample). We also ran four blanks to test for analytical consistency. For each sample/blank we ran three cycles (5 min static, 90 secs purge for each cycle). The extracted lipids were dried with nitrogen gas, further dissolved and fractionated with Aluminum oxide column chromatography to separate non-polar (4 ml 9:1 Hexane:DCM), ketone (4 ml 1:1 Hexane:DCM), and polar lipids (4 ml 1:1 DCM:MeOH). The Alumina column was made with 7.5g Al_2O_3 covered with 2.5g Na_2SO_4, held with a small amount of glass wood at the end of the column, and filled with 9:1 Hexane:DCM.

Since *n*-alkenes are also extracted and mixed with *n*-alkanes in nonpolar extractions, we then ran a silver-nitrate-infused silica gel column to separate *n*-alkenes from the *n*-alkanes (Patalano et al., 2020). The silver nitrate column was composed of 0.5g 10% $SiAgNO_3$ covered with 0.5g activated silica gel (Grade 923) and washed with 4ml hexane. In total, 10g 10% $SiAgNO_3$ was prepared for the column with 59 ml silver nitrate solution (0.1N) and 10g activated silica gel (Grade 923), stored in a drying oven at 75 °C until all water had evaporated. Identification and quantification of saturated *n*-alkanes were achieved using an Agilent Technologies 7890B GC system and Agilent Technologies 5977B MSD in electron impact (EI) mode using selected ion monitoring (SIM). The mass range for SIM was m/z 85. The column we used was the Agilent Technologies column (HP-5MS, 60 m x 250 μm x 0.25 μm). The GC oven temperature was isothermal for 2.5 min at 50°C and then programmed from 50 to 310°C at 16°C/min. For the front injector, the syringe size was 5 μl, and the injection volume was 1 μl. More detailed settings are provided in Appendix A.

Here, we focused on the long-chain *n*-alkanes (>= C_{19}) in the surface sediment to evaluate their ability to distinguish the proportions of grasses and higher vascular plants in lake catchments. I analyzed the C_{19} – C_{35} *n*-alkanes which provided ratios of individual *n*-alkane abundances. I also applied another two indices, the average chain length (ACL) and the carbon preference index (CPI), to enhance our ability to characterize the *n*-alkane distribution in sediments. ACL is the weighted average

carbon number of *n*-alkanes in each sample, which may be useful as an indicator of the organic matter sources to sediment (aquatic vs terrestrial), and it is expressed as

$$ACL = SUM\ (C_n \times n) / SUM\ (C_n),$$

where n is the number of carbon atoms, and C_n is their concentration in the sample. CPI represents the predominance of the odd/even carbon ratio of the *n*-alkanes and is expressed as:

$$CPI = [SUM_{odd}(C_{21}\text{-}C_{33}) + SUM_{odd}(C_{23}\text{-}C_{35})]/(2SUM_{even}C_{22}\text{-}C_{34}),$$

which is to quantify the odd/even ratio of the *n*-alkanes (in μg/g) carbon numbers, and to capture the level of odd *n*-alkane dominance (Marzi et al., 1993). Long chain *n*-alkanes with CPI greater than 1 suggest the *n*-alkane sources are weighted to more terrestrial plants relative to aquatic plants. We analyzed the concentrations of *n*-alkanes in lake sediment as well as their ACL and CPI to characterize differences in carbon sources to lake sediments among the different ecoregions.

2.3.2 Lignin-derived phenols

The residues in the ASE cells from the *n*-alkane analysis were packed and sent to our collaborators (at the University of Toronto in Scarborough) for lignin-derived phenols and alkanoic acid analysis. The dried samples (around 0.5 g each) were packed and sent to the University of Toronto at Scarborough for the lignin-derived phenols isolation and analysis using CuO oxidation (Otto, Shunthirasingham, et al., 2005). 0.5 g of dried sample was first mixed with 1g of CuO, 100mg of ammonium iron (II) sulfate hexahydrate [$Fe(NH_4)_2\ (SO_4)_2 \cdot 6H_2O$], and 15 mL of 2 M sodium hydroxide.

We then loaded a Teflon-lined bomb with the mixture, purged with N_2 gas and heated at 170 °C for 2.5 hours, the extracts were transferred to another Teflon tube. We then added 10 ml of deionized water to the residues, sonicated each sample for 15 minutes, then centrifuged, and combined with other supernatants in Teflon tubes (repeated twice). We then acidified the supernatants to pH 1 with hydrochloric acid and kept extracts in the dark at room temperature for an hour to prevent the polymerization of cinnamic acids. Samples were then centrifuged for 30 min at 2500 rpm and supernatants were collected. Supernatants were then extracted by solid-phase extraction, and eluted three times with 0.5 mL of dichloromethane:methylacetate:pyridine (70:25:5, v:v:v), followed by 0.5 mL of methanol (twice). We then dried the CuO oxidized products with anhydrous sodium sulfate and N_2 gas. The soil extracts were then derivatized prior to gas chromatography-mass spectrometry (GC-MS) analysis (Man et al., 2022; Otto & Simpson, 2006).

2.3.3 Delta ^{13}C and C/N ratio analysis

Carbon and nitrogen elemental and isotopic analysis for the sediments of the sampled lakes was performed at the Jan Veizer Stable Isotope Laboratory (Ottawa, Ontario). Prior to the organic carbon and $\delta^{13}C$ analysis, we removed the carbonates from the sediment by acid fumigation. We added a few drops of distilled water to the dried sediment in the glass scintillation vial, then acidified samples by HCl fumes in an acid desiccator for 24 hours. To rinse the acidified sediment, we filled 3/4 of the vial with

distilled water, left it for one day to settle, and then removed the overlying water (leaving 1 to 2 mm above the surface the of sediment). We then rinsed the sediment until the pH ~ 7. Acidified sediment samples were weighed out for isotopic analysis into tin capsules with Tungstic oxide (WO_3, pre-heated overnight at 900 °C to remove organic residues). The capsules were then flash combusted at 1800°C in an Elementar Vario EL Cube elemental analyzer. The resulting gases were carried by Ultra-pure helium through the column and obtained N_2, CO_2, H_2O, and SO_2, then separated by "trap and purge" method. Details are provided in Appendix B.

2.3.4 Lake trophic level analysis

Surface water samples were collected using a 2 L Limnos closing water sampler (Limnos, Poland). The collected water sample was subsampled immediately for total phosphorus (TP) and total nitrogen (TN) into acid-washed plastic vials. The subsample for dissolved organic carbon (DOC) was filtered through pre-combusted Whatman GF/F filters (nominal pore size 0.7 μm) before being stored in acid-washed, brown glass bottles without head space. For chlorophyll *a*, three replicates of 500 ml water sample were filtered onto Whatman GF/F filters and stored frozen for later analysis.

TP, TN, and DOC were analyzed by the GRIL-Université du Québec à Montréal (UQAM) analytical laboratory in Montreal following standard protocols (McKenna & Doering, 1995; Patton & Kryskalla, 2003; Wetzel & Likens, 2000). Chlorophyll-a (Chl-a) was extracted with hot ethanol, after which the extracts were filtered through

pre-combusted Whatman GF/F filters (0.2 μm) and analyzed with a Cary Eclipse spectrofluorometer (Agilent Technologies) at UQAC following Nusch (1980). The extracts were scanned before and after acidification to subtract phaeopigments.

2.4 Watershed delineation

2.4.1 Watershed boundary generation

We delineated watershed boundaries using the *flow direction* and *flow accumulation* functions in ArcGIS Pro (version 3.1). We used the Canadian digital elevation model (CDEM, 30m resolution) to generate the flow direction and accumulation layers, which presented the accumulated weight of all cells flowing into the nearest downslope cell (Canadian Digital Elevation Model, 1945-2011 - Open Government Portal). D8 was the flow direction method used and the output data type for *flow accumulation* was float (floating point type). D8 flow direction is defined as the direction of flow from one cell to one of its eight adjacent or diagonal neighbors with the steepest downward slope. Each individual *pour point* was set at the highest accumulation value on the lake outline which depended on the different flow accumulation patterns of the area surrounding the lake. The latter was different for every sampled lake due to the varying topography. Then the resulting catchment outline from the *watershed* function was overlayed on the 2019 Global Land Cover data (Buchhorn et al., 2020). The Global land cover (100m resolution) included a total of 21 land cover types for open forest, closed forest, and other land cover. For both open and closed forests, land cover types included evergreen needle-leaved,

deciduous needle-leaved, evergreen broadleaved, deciduous broadleaved, mixed type, and unknown type. Other land covers considered were shrubland, herbaceous vegetation/wetland, moss and lichen, bare/sparse, cropland, built-up, snow and ice, and permanent water bodies. The ratio of each land cover type was calculated and compared with our *n*-alkane dataset for estimating the ability of *n*-alkanes to represent the relative proportions of land cover types. The watershed boundaries generated based on the CDEM were named Accumulation maps. We also generated zones using the *buffer* function in ArcGIS, which represented the lake shape expanded by 1 km from the shoreline, which we named Buffer maps. The combination of each lake Accumulation map and Buffer map was named the Combined map.

2.4.2 Data collection

We specified the land cover composition of pixels in our generated watershed boundary into shrub, herb vegetation, herb wetland, bare/sparse, evergreen needle-leaved close/open forest, deciduous broadleaved close/open forest, mixed close forest, and unknown close/open forest. Details for the pixel number of each land cover type for sampled lakes are available in Table S1. For this analysis, all pixels referring to forests and shrubs were combined under the 'Woody plant' category, and herb vegetation and herb wetlands pixels were combined under the 'Herbaceous plant' category. The Herbaceous to Woody plant ratio (shorten as H/W ratio) was calculated by dividing the number of Woody plant pixels by the sum of the Woody and Herbaceous plant pixels for Accumulation, Buffer, and Combined maps. Then we did

the same calculation for *n*-alkane concentrations, where the *n*-alkanes that predominate in trees and shrubs (C_{27}, C_{29}), were compared with the *n*-alkanes that predominate in grasses and herbs (C_{31}), as follows: $C_{31}/(C_{27} + C_{31})$, $C_{31}/(C_{29} + C_{31})$, and $C_{31}/(C_{27} + C_{29} + C_{31})$.

2.5 Data analysis

For all the biomarkers we tested, we calculated the mean and SD for each ecoregion and used one-way ANOVA to analyze the variance difference between ecoregions. We also performed regression analysis to compare our alkane ratios with the H/W ratios from the generated watershed boundaries and determined whether the *n*-alkane composition was correlated with land cover estimates of the lake's watersheds. A $p<0.05$ was considered significant for regression analysis and one-way ANOVA.

Chapter 3 Results and Discussion

3.1 Trophic status of studied lakes

The study lakes ranged from oligotrophic to hypereutrophic (Table 3.1) based on the concentration of total phosphorus (TP) and Trophic Status Index based on chlorophyll a (TSI (Chl-a)). All the TN/TP ratios for the studied lakes were >7.2 by mass, suggesting phosphorus as the limiting nutrient for algal growth in these lakes according to the Redfield ratio (Abell et al., 2010; Redfield et al., 1963). The mean TP was 22.24µg/L (±10.85 SD) for Boreal Upland-North lakes, 16.79µg/L (±11.52 SD) for Boreal Upland-South lakes, 20.40µg/L (±10.81 SD) for Boreal Transition lakes, 52.49µg/L (± 69.33 SD) for Aspen Parkland lakes, and 115.34µg/L (± 119.53 SD) for Prairie Grassland lakes. Although TP in lakes ranged from 7.76 µg/L to 251.28µg/L, comparisons of the ecoregions by one-way ANOVA didn't find differences among the ecoregions ($p=0.228$. $F_{(4, 13)}=1.62$). We further log-transformed the data to reduce the large differences in variance among ecoregions, and the ANOVA produced a $p=0.16$ and $F_{(4, 13)}=1.99$, which still showed no significant difference in TP among ecoregions. Thus factors other than ecoregion appear to influence TP concentrations.

We also calculated the Trophic Status Index (TSI) based on chlorophyll *a* (Chl-*a*) (Carlson, 1977) to be 51.88 (±3.62 SD) for Boreal Upland-North lakes, 41.38 (±10.51 SD) for Boreal Upland-South lakes, 49.06 (±5.81 SD) for Boreal Transition lakes, 53.54 (± 12.34 SD) for Aspen Parkland lakes, and 47.58 (± 9 SD) for Prairie Grassland lakes. The one-way ANOVA for both the raw data and log-transformed data

showed no significant difference in TSI (Chl-*a*) among ecoregions (p-value was 0.39 and 0.3, and $F_{(4, 14)}$ was 1.12 and 1.34, respectively).

Based on TP, the results suggest that most of the lakes were meso-eutrophic (Wetzel, 2001). However, Amber Lake was classified as oligo-mesotrophic, while Twin Lake and Antelope Lake were hypereutrophic. The TSI (Chl-*a*) results indicated that most lakes were mesotrophic or eutrophic, except for Twin Lake (hypereutrophic), Jeannette Lake (oligotrophic), and Zeden Lake (oligotrophic). Overall, the TP results were generally consistent with the TSI (Chl-*a*). The hypertrophic status in Twin Lake was shown by both methods, which may be the result of the farmland in the catchment area, which is associated with eutrophication elsewhere (e.g. Keatley et al., 2011). In contrast, Antelope Lake's trophic status varied between the two methods, its high phosphorus concentration was likely caused by the use of fertilizers by farms in the catchment. However, the low chlorophyll-*a* concentration and low TSI (Chl-*a*) suggest that Antelope Lake didn't have very high algal productivity. The previous studies showed that Antelope Lake had a high salinity with a conductivity of 8.4, which could negatively influence algae growth (Hammer, 1978; Shetty et al., 2019). Other than salinity, Antelope Lake looked turbid during the sampling, which suggests light limitation could be another factor that caused low algae production in Antelope Lake (Bouterfas et al., 2002; Ganf & Oliver, 1982).

Table 3.1. Summary of the trophic status of sampled Saskatchewan Lakes. Chl-a Ave is the average chlorophyll-a concentration (µg/L). DOC is the dissolved organic carbon (mg/L). TN is the total nitrogen (mg/L). TP is the total phosphorus (µg/L). TSI(Chl-a) is the trophic Status Index calculated using Chl-a values.

Sample lakes Ecoregion	Amber BU (North)	Bray BU (North)	Fontaine BU (North)	Sinclair BU (North)	Heritage BU (South)	Jeannette BU (South)	McPhee BU (South)	Zeden BU (South)	Eagle BT	Jimmy BT
Chl-a Ave	8.95	6.90	6.56	14.67	4.21	1.06	11.63	1.58	12.17	7.13
DOC	1.17	2.89	2.20	8.22	11.65	7.57	15.98	5.62	21.27	22.71
TN	0.18	0.53	0.48	0.64	0.63	0.48	0.63	n.a.	1.87	1.27
TP	7.76*	23.41**	34.08***	23.69**	11.03**	11.38**	27.95**	n.a.	36.26***	15.12**
TN/TP	23.64	22.83	14.04	26.92	57.00	42.09	22.43	n.a.	51.65	83.79
TSI(Chl-a)	52.07	49.52	49.02	56.92	44.68	31.13	54.64	35.07	55.08	49.84

Sample lakes Ecoregion	Matheson BT	Pêche BT	Dillberry AP	Picnic AP	Suffern AP	Twin AP	Antelope PG	Clearwater PG	Pelletier PG
Chl-a Ave	2.93	7.39	3.33	6.54	8.36	61.99	3.94	2.87	16.08
DOC	17.48	11.90	12.36	14.14	10.12	14.52	45.15	26.27	10.26
TN	1.26	0.84	0.89	1.19	0.79	2.04	3.11	1.71	1.33
TP	17.87**	12.33**	16.10**	21.22**	16.21**	**156.42**	**251.28**	68.11***	26.64**
TN/TP	68.27	70.56	55.46	56.25	13.05	48.65	12.38	25.14	49.74
TSI(Chl-a)	50.18	41.12	42.37	48.99	51.40	71.06	44.01	40.91	57.82

BU-Boreal Plain Upland, BT-Boreal Transition, AP-Aspen Parkland, PG-Prairie Grassland.
*Oligo-mesotrophic, **Meso-eutrophic, ***Eutrophic, bolded - Hypereutrophic
TSI(Chl-a) = 10 (6 - (2.04 - 0.68lnChl-a) / ln2)
n.a. Sample lost

3.2 n-alkane analysis

3.2.1 Composition of n-alkanes in lake sediments

We compared the composition of *n*-alkanes in lake sediments among ecoregions to determine if lake and catchment characteristics (especially land cover type) affected them. We considered the C_{19} – C_{35} *n*-alkanes for sediments in all 19 lakes (Table 3.2, Fig. S2). The carbon preference index (CPI), which is related to the relative contributions of terrestrial/aquatic plant sources based on the predominance of odd/even carbon ratio of the *n*-alkanes, was greater than 1 in all the collected samples for C_{21}-C_{33} *n*-alkanes (Table 3.2), indicating the long-chain *n*-alkanes likely derive from a predominance of terrestrial higher plants (relative to aquatic plants) in sedimented materials (Collister et al., 1994; Marzi et al., 1993).

Average chain length (ACL) is the weighted average carbon number of *n*-alkanes in the sediment, calculated from C_{23} to $C_{35,}$ and is generally consistent with the carbon number maxima (C_{max}) (Simoneit et al., 1991). C_{27} and C_{29} alkanes are generally most prevalent in the waxes of trees and shrubs, in contrast to grasses that are dominated by C_{31} (Bliedtner et al., 2018; Cranwell I et al., 1987; Cranwell, 1973; Struck et al., 2020). As shown in Table 3.2, Boreal Upland-South, Boreal Transition, and Aspen Parkland had an ACL of around 27 which is consistent with the previous studies and the forest-dominated land cover around the lakes (Table S1). However, Boreal Upland-North and Prairie Grassland had lower ACLs than expected for trees or

grassed dominated areas. For Boreal Upland-North lakes (Amber Lake, Bray Lake, and Fontaine Lake) ACLs were very low considering their forest-dominated areas. These low ACLs may be the result of low amounts of fallen litter by the coniferous trees that predominate in these areas, resulting in undetectable concentrations of *n*-alkanes from C_{25} to C_{35} that would normally derive from terrestrial litter. The ACLs in Prairie Grassland lakes were also lower than our expectation (around 31 for grasses), which may be caused by inputs from agriculture in the catchment area because certain grains like wheat contain a high proportion of C_{27} and C_{29} (Liu et al., 2016). The C/N ratios ranged from 7.78 to 13.35 (mean = 9.89, SD = 1.21), which were generally between phytoplankton and terrestrial plants (Table 3.1).

Table 3.2. Parameters of *n* -alkanes and stable isotopes of carbon in the Saskatchewan Lake samples. C_{max} is the carbon number of n-alkane with the highest concentration. ACL is the weighted average carbon number of n-alkanes in each sample. CPI value is the index to determine the predominance of the odd/even carbon ratio of the *n* -alkanes.

Sample lakes	Amber	Bray	Fontaine	Sinclair	Heritage	Jeannette	McPhee	Zeden	Eagle	Jimmy
Ecoregion	BU (North)	BU (North)	BU (North)	BU (North)	BU (South)	BU (South)	BU (South)	BU (South)	BT	BT
n-C range	19-35	19-35	19-35	19-35	19-35	19-35	19-35	19-35	19-35	19-35
C_{max}	C_{23}	C_{23}	C_{23}	C_{27}	C_{27}	C_{27}	C_{27}	C_{27}	C_{27}	C_{27}
ACL	23.04	23.00	23.94	26.03	26.73	26.70	27.00	27.50	26.37	26.92
CPI	5.78	3.19	4.73	4.94	6.55	9.17	4.79	6.00	2.17	4.48
$\delta^{13}C$	-33.35	-25.39	-26.92	-32.23	-30.72	-28.73	-33.87	-29.33	-31.00	-30.56
C/N	10.36	10.13	10.20	10.21	13.35	9.64	10.37	9.35	9.77	10.19
$C_{31}/(C_{27} + C_{31})$	n.a.	n.a.	n.a.	0.05	0.21	0.20	0.27	0.31	0.14	0.24
$C_{31}/(C_{29} + C_{31})$	0	n.a.	n.a.	0.11	0.33	0.37	0.36	0.39	0.17	0.28
$C_{31}/(C_{27} + C_{29} + C_{31})$	0	n.a.	n.a.	0.04	0.15	0.15	0.18	0.21	0.08	0.15

Sample lakes	Matheson	Pêche	Dillberry	Picnic	Suffern	Twin	Antelope	Clearwater	Pelletier
Ecoregion	BT	BT	AP	AP	AP	AP	PG	PG	PG
n-C range	19-35	19-35	19-35	19-35	19-35	19-35	19-35	19-35	19-35
C_{max}	C_{27}	C_{27}	C_{27}	C_{27}	C_{27}	C_{27}	C_{29}	C_{29}	C_{29}
ACL	26.37	26.72	27.45	27.34	26.93	27.47	27.99	27.75	27.80
CPI	4.03	4.01	4.97	10.00	4.21	5.77	219.54	14.35	3.83
$\delta^{13}C$	-28.67	-32.44	-24.39	-25.28	-29.39	-27.98	-25.58	-18.24	-24.07
C/N	10.66	9.40	10.21	10.98	9.19	9.80	7.78	7.84	8.49
$C_{31}/(C_{27} + C_{31})$	0.16	0.21	0.32	0.30	0.22	0.33	0.50	0.35	0.48
$C_{31}/(C_{29} + C_{31})$	0.31	0.32	0.35	0.33	0.31	0.40	0.43	0.25	0.33
$C_{31}/(C_{27} + C_{29} + C_{31})$	0.12	0.14	0.20	0.19	0.15	0.22	0.30	0.17	0.24

BU-Boreal Plain Upland, BT-Boreal Transition, AP-Aspen Parkland, PG-Prairie Grassland.
n.a. Concentration of C_{27}, C_{29}, and C31 was not detected, removed from analysis.

3.2.2 n-alkane comparisons between ecoregions

We produced a series of ratios between C_{27}, C_{29}, and C_{31} as proxies of the relative proportion of herbaceous plants and woody plants (Schefuß et al., 2003; Schwark et al., 2002; Zhang et al., 2008), and to determine whether significant differences in *n*-alkane composition exist among ecoregions (Table 3.2). Here we calculated the ratio of the C_{31} *n*-alkane to (C_{27} + C_{31}), (C_{29} + C_{31}), and (C_{27} +C_{29} + C_{31}) as three separate proxies (referred to as $Ratio_{27}$, $Ratio_{29}$, and $Ratio_{27+29}$, respectively) in the studied lake sediments (Table 3.2).

We observed significant differences between ecoregions using a one-way ANOVA test for $Ratio_{27}$, $Ratio_{29}$, and $Ratio_{27+29}$ (p-value = 0.0002, 0.0005, and 0.0004, respectively) (Fig. 3.1). Overall, Boreal Upland-North had a lower ratio than the other ecoregions for all three ratios, while Boreal Upland-South and Aspen Parkland did not show a significant difference in all three ratios (Table 3.2, Fig. 3.1). This result is consistent with the land cover of Boreal Upland-North watersheds that are dominated by forests and shrubs with a low proportion of herbaceous plants. Prairie Grassland had a significantly higher $Ratio_{27}$ than the other ecoregions, and a significantly higher $Ratio_{27+29}$ than Boreal Transition, but no significant difference was shown for $Ratio_{29}$ (Fig. 3.1). This may be due to the *n*-alkane contributions from crops in Prairie Grassland lakes, which may have increased the C_{29} concentration in the lake sediments (Fig. S2). The herbaceous plants in the watersheds of Boreal Transition and

Aspen Parkland could also increase the concentration of C_{31} and lead to an overlapping range of $Ratio_{29}$ with Prairie Grassland.

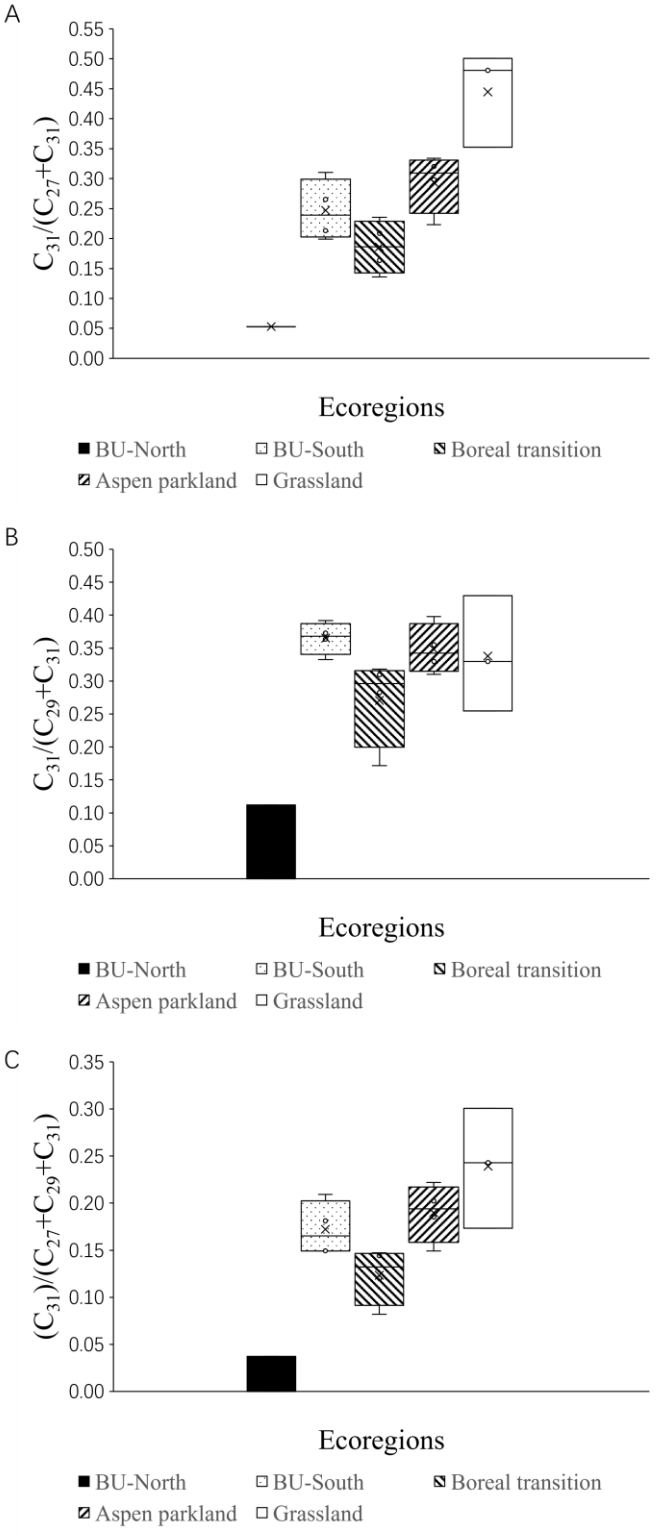

Fig. 3.1. The ratio of the C_{31} *n*-alkane to (A) (C_{27} + C_{31}), (B) (C_{29} + C_{31}), and (C) (C_{27} +C_{29} + C_{31}) *n*-alkanes for the four ecoregions, p-value = 0.0002, 0.0005, and 0.0004, respectively.

3.2.3 n-alkane and land cover correlations

To date, most of the studies on *n*-alkanes as biomarkers are focused on plant tissues like leaves and grasses collected at the watershed of target lakes. The complexity of the watershed land cover composition could decrease the reliability of designated ecoregions as accurate descriptors of lakes in our analysis. As shown in Table S1, the land cover proportion of herbaceous, shrubs, and evergreen/deciduous trees in each lake's watershed boundary is variable, even within each ecoregion. Given that land cover maps and digital elevation maps are more accurate descriptions of individual lakes and have been recently updated to show current vegetation cover, we also used land cover maps to relate the sediment composition of *n*-alkanes directly to the land cover of each individual lake. We quantified the different land cover categories for each lake's catchment (called the Accumulation map), and we also defined land cover within a 1 km distance of the lake's shoreline (called the Buffer map). The combined Accumulation and Buffer maps were also considered (called the Combined map). For simplicity, we defined the combined shrub, evergreen forest, and deciduous forest categories as Woody plant cover and we combined herbaceous vegetation and wetland as Herbaceous plant cover.

We calculated the ratio of Herbaceous to Woody plant areal extent (H/W ratio) in Accumulation, Buffer, and Combined maps of each of the lakes. We then correlated these areas with $Ratio_{27}$, $Ratio_{29}$, and $Ratio_{27+29}$ (Fig. 3.2, Table 3.3, and Fig. S1). Some lakes (Amber Lake, Bray Lake, and Fontaine Lake) had sediments with

undetectable C_{27}, C_{29}, or C_{31}, and were therefore removed from the analysis. Overall, the regression analysis showed that the H/W ratio was positively correlated with $Ratio_{27}$ and $Ratio_{27+29}$ (Table 3.3), and a post hoc Tukey's test showed that correlations with $Ratio_{27}$ were significantly higher than $Ratio_{27+29}$ at p-value<0.05. In contrast, we observed no significant correlation between the H/W ratio and $Ratio_{29}$ (Table 3.3). Moreover, the regression between the H/W ratio and $Ratio_{27}$ had the highest R^2 of 0.549 and therefore the best fit. This result suggests that C_{27} is a relatively more representative *n*-alkane to reflect the relative proportions of herbaceous plants and woody plants in sediment, whereas C_{29} is less representative, at least based on this set of data. For all regressions, Combined maps always had the highest R^2 (Table 3.3), suggesting this approach of calculating land cover was the best predictor of *n*-alkane composition in sediment (Fig. 3.2). The regression analysis between Chl-*a* and *n*-alkanes showed no significant correlation (Table 3.3), which further supported the notion that the *n*-alkane ratios reflected land cover and not autochthonous (algal) production in the lakes.

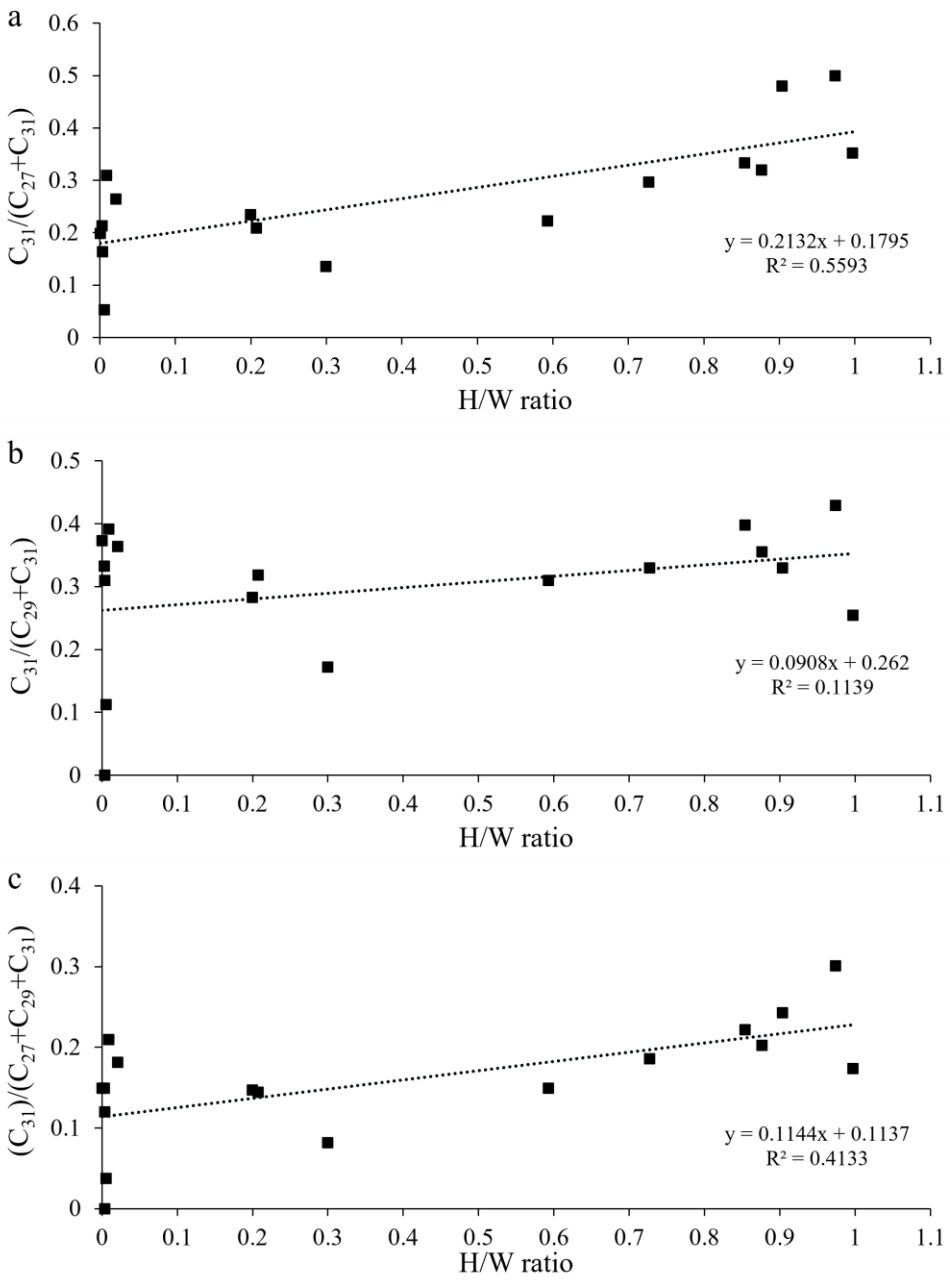

Fig. 3.2. Linear regression between Herbaceous to Woody plants relative ratio (H/W ratio) and (A) $C_{31}/(C_{27}+C_{31})$, (B) $C_{31}/(C_{29}+C_{31})$, and (C) $C_{31}/(C_{27}+C_{29}+C_{31})$ for Combined maps.

Table 3.3. Summary of regression analysis between Herbaceous to Woody plants relative ratios (H/W ratio) and *n*-alkane relative ratios for Accumulation, Buffer, and Combined maps, and regression analysis between *n*-alkane relative ratios and chlorophyll *a* concentration (Chl-a).

Regression	R^2	Standard Error	df (Regression)	df (Residual)	F	p-value	Correlation
H/W ratio vs. $C_{31}/(C_{27} + C_{31})$							
Accumulation	0.533	0.083	1	14	16.003	0.0013*	0.73
Buffer	0.554	0.081	1	14	17.422	0.0009**	0.74
Combined	0.559	0.080	1	14	17.769	0.0009**	0.75
H/W ratio vs. $C_{31}/(C_{29} + C_{31})$							
Accumulation	0.111	0.107	1	15	1.870	0.1917	0.33
Buffer	0.086	0.109	1	15	1.419	0.2521	0.29
Combined	0.114	0.107	1	15	1.929	0.1852	0.34
H/W ratio vs. $C_{31}/(C_{27} + C_{29} + C_{31})$							
Accumulation	0.398	0.058	1	15	9.921	0.0066*	0.63
Buffer	0.381	0.059	1	15	9.214	0.0083*	0.62
Combined	0.413	0.058	1	15	10.567	0.0054*	0.64
Chl-a vs. *n*-alkanes ratios							
Chl-a vs. $C_{31}/(C_{27} + C_{31})$	0.010	0.120	1	14	0.147	0.7067	0.10
Chl-a vs. $C_{31}/(C_{29} + C_{31})$	0.006	0.114	1	15	0.090	0.7686	0.08
Chl-a vs. $C_{31}/(C_{27} + C_{29} + C_{31})$	0.015	0.075	1	15	0.224	0.6428	0.12

*p-value < 0.05, **p-value < 0.001, ***p-value < 0.0001

3.3 Carbon isotopic compositions

As shown in Fig. 3.2A, the C/N ratio ranges from 7.78 to 13.35 (mean = 9.89, SD = 1.21), which suggests high contributions from autochthonous production. This result is possibly due to the high productivity in the studied lakes as shown by the high chlorophyll *a* concentrations and meso/eutrophic conditions (TP, Table 3.1). Especially for Prairie Grassland, the lakes had a significantly lower C/N ratio (mean = 8.04, SD = 0.40) than other ecoregions which corresponds to the high nutrient concentrations. For the other ecoregions, the one-way ANOVA test showed that there was no significant difference in the C/N ratio between ecoregions ($p=0.78$, $F_{(3, 12)}=0.36$) which is generally could be explained by the meso-eutrophic nutrients in the

lakes.

Other than C/N ratio, the mean $\delta^{13}C$ was -29.47 (±3.91 SD) for Boreal Upland-North lakes, -30.66 (±2.30 SD) for Boreal Upland-South lakes, -30.66 (±1.56 SD) for Boreal Transition lakes, -26.76 (±2.33 SD) for Aspen Parkland lakes, and -22.63 (±3.88 SD) for Prairie Grassland lakes. Here we observed the highest mean $\delta^{13}C$ in Prairie Grassland lakes. However, the range fell into the range of C3 plants ($\delta^{13}C$ around -25 to -30) and overlapping with Aspen Parkland, suggests that $\delta^{13}C$ is not able to separate Prairie Grassland from other forest ecoregions (Fig. 3.3). A possible reason for this lower $\delta^{13}C$ is the contamination from the wheat farming (C3 plant) in the Prairie Grassland which caused the unexpected lower $\delta^{13}C$ results. Despite the Prairie Grassland, the $\delta^{13}C$ of forest ecoregions were overlapping with each other, and the one-way ANOVA showed that there is no significant difference between Aspen Parkland, Boreal Transition, and Boreal Upland ($p=0.18$, $F_{(3.\ 12)}=1.91$).
The differences between C3 and C4 plants based on their carbon fixation pathways lead to significantly higher $\delta^{13}C$ on the C3 plant leaf wax than in C4 plants (Chikaraishi et al., 2004; Collister et al., 1994; Duan et al., 2004; O'Leary, 1988; Rieley et al., 1993). In addition, the C/N ratio was used to distinguish between terrestrial and aquatic organic matter. The plot between $\delta^{13}C$ and C/N ratio is then used as a proxy to determine the biomaterial source (Meyers, 2003).

The differences between C3 and C4 plants based on their carbon fixation pathways

lead to significantly higher $\delta^{13}C$ on the C3 plant leaf wax than in C4 plants (Chikaraishi et al., 2004; Collister et al., 1994; Duan et al., 2004; O'Leary, 1988; Rieley et al., 1993). In addition, the C/N ratio was used to distinguish between terrestrial and aquatic organic matter. The plot between $\delta^{13}C$ and C/N ratio is then used as a proxy to determine the biomaterial source (Meyers, 2003). In this study, the plot between $\delta^{13}C$ and C/N ratio is insufficient to determine the biomaterial source, especially under the effect of high autochthonous production.

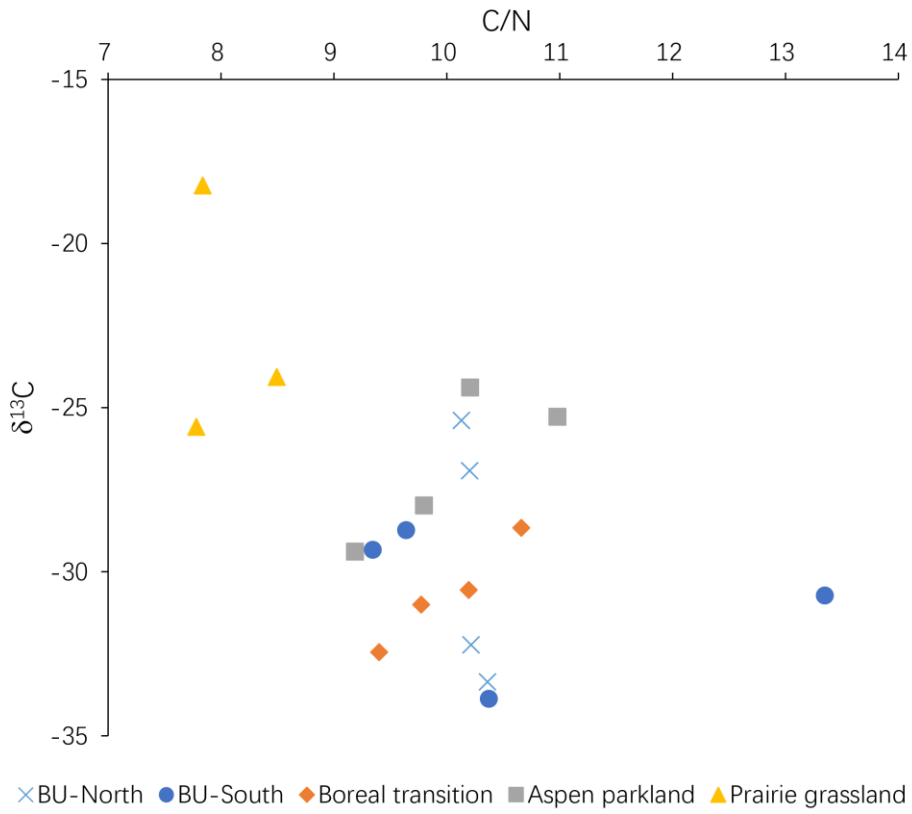

Fig. 3.3. $\delta^{13}C$ versus C/N ratio of the four ecoregions in Saskatchewan from north to south.

3.4 Lignin-derived phenols compositions

Lignin-derived phenols composition of the sampled lakes is summarized in Fig.

3.4.A. Boreal Upland is characterized by angiosperm nonwoody and gymnosperm nonwoody plants. These S/V values fell into our expected range, but C/V values were higher than our expectations. For both north and south Boreal Upland, the watersheds of sampled lakes were dominated by evergreen needle-leaved trees like conifers, but with some unknown types of forest (Table S1). These unknown-type forests may include angiosperms like trembling aspen (deciduous broad-leaved), and the higher C/V value may result from the fallen aspen leaves (angiosperm nonwoody tissue). In Boreal Upland-South, Jeannette Lake and Zeden Lake had much higher C/V values than the expected angiosperm nonwoody range (Fig. 3.4A). These ratios may be affected by degradation either before or after they deposited into sediment may have altered these structures. Since carboxylic acid is oxidized from aldehyde, we further analyzed the ratio between carboxylic acid (Ad) and aldehyde (Al) of vanillyl and syringyl to reflect the degradation (Fig. 3.4.B, C), whereas increasing Ad/Al indicates more degradation in the material (Ertel & Hedges, 1984; Hedges et al., 1988; Vane et al., 2003). The mean $(Ad/Al)_v$ was 1.62 (±0.81 SD) for Boreal Upland-North lakes, 1.93 (±0.45 SD) for Boreal Upland-South lakes, 1.77 (±0.11 SD) for Boreal Transition lakes, 1.59 (±0.25 SD) for Aspen Parkland lakes, and 1.80 (±0.36 SD) for Prairie Grassland lakes. The mean $(Ad/Al)_s$ was 1.40 (±0.39 SD) for Boreal Upland-North lakes, 1.14 (±0.20 SD) for Boreal Upland-South lakes, 1.07 (±0.0.22 SD) for Boreal Transition lakes, 1.17 (±0.05 SD) for Aspen Parkland lakes, and 1.01 (±0.12 SD) for Prairie Grassland lakes. The ANOVA test showed no significant difference between ecoregions for $(Ad/Al)_v$ ($p=0.89$, $F_{(4,12)}=0.27$)and $(Ad/Al)_s$ ($p=0.38$, $F_{(4,9)}=1.18$), and

the results suggested high degradation in the lake sediments, where some lakes had all aldehyde degraded to carboxylic acid (blanks in Fig. 3.4.B, C). This degradation of vanillyl may cause the increasing C/V value for Jeannette Lake and Zeden Lake.

Boreal Transition and Aspen Parkland also fell into the angiosperm nonwoody range, the C/V value also higher than our expectation which the high proportion of deciduous broad-leaved trees could cause these results. An exception in the Boreal Transition is Matheson Lake, in which the S/V value was much lower than other lakes. As shown in Table S1, the watershed of Matheson Lake had a higher proportion of evergreen needle-leaved trees than deciduous broad-leaved trees, which could be the reason for its low S/V value. Prairie Grassland, which is dominated by herbivorous vegetation/wetland, fell into the angiosperm nonwoody range as we expected.

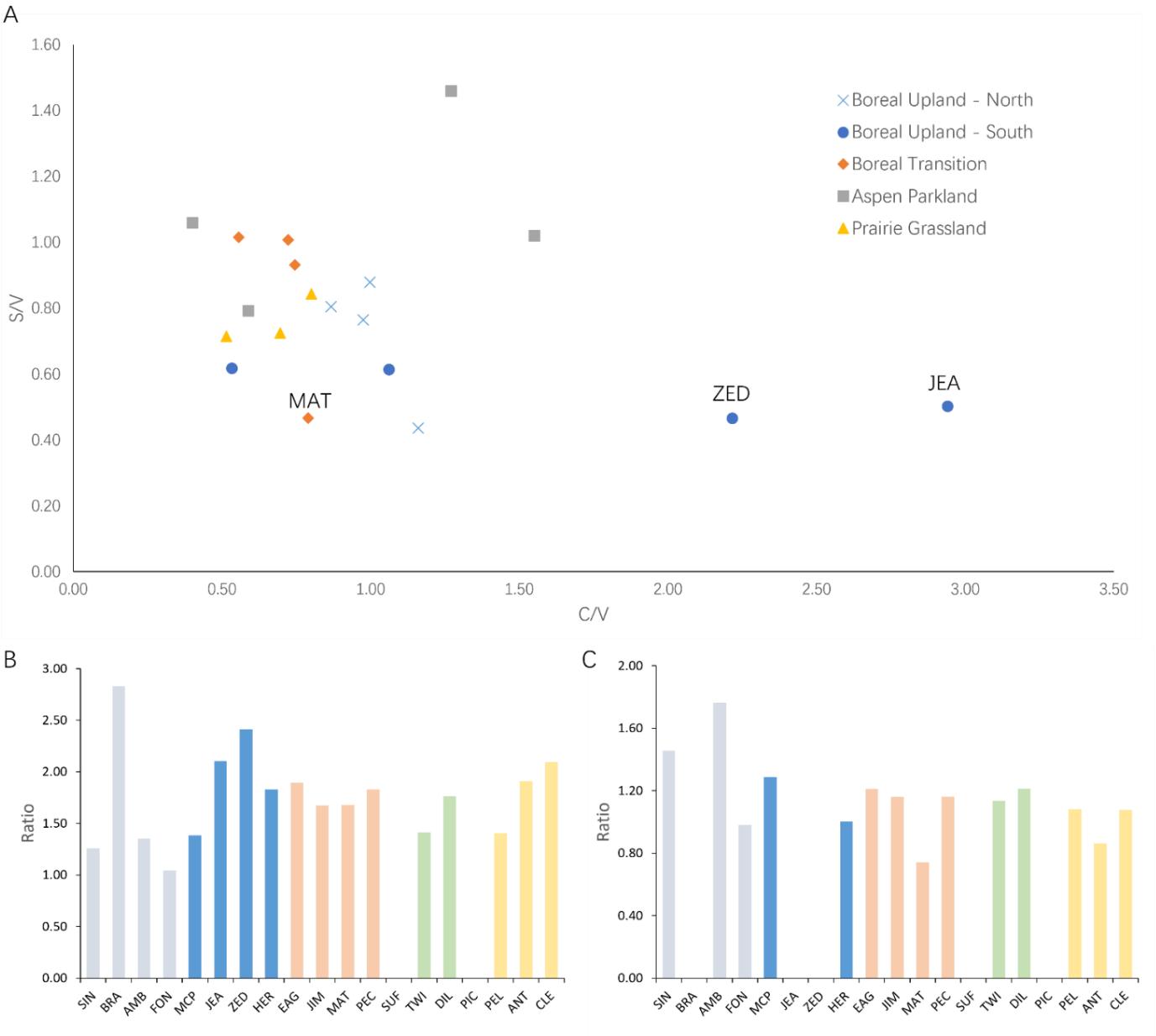

Fig. 3.4. Lignin derived phenol composition of studied samples, (A) present as syringyls/vanillyls vs. cinnamyls/vanillyls. Ratio of carboxylic acid (Ad) to aldehyde (Al) forms of the lignols (Ad/Al) for (B) vanillyls and (C) syringyls in the studied sample. Blanks in B and C means no aldehyde detected.

Chapter 4 Conclusion

We studied 19 lake sediment cores in Saskatchewan across the following ecoregions: Prairie Grassland, Aspen Parkland, Boreal Transition, and Boreal Upland, with lakes spanning latitudes from 49° to 59°N. This large spatial and ecological scale provided an opportunity to analyze the different biomarker compositions among and within ecoregions. Overall, the lakes were mesotrophic to eutrophic, with some exceptions due to agriculture-induced hyper-eutrophication, lake salinity, or light limitation. The ACL values showed significant differences between ecoregions, where the lower ACL for Prairie Grassland suggesting high autochthonous production may have been influenced by nutrients from agriculture in some parts of Saskatchewan. The ratio $C_{31}/(C_{27}+C_{31})$ showed the strongest positive correlation with the ratio of herbaceous to woody plants (H/W) in the catchments. This strong correlation revealed the potential to approximate changes in land cover (particularly related to tree line) based on the *n*-alkane composition of lake sediments. The C/N ratio suggested major contributions of autochthonous (algal) production to bulk sediment organic matter, but CPI estimates of *n*-alkanes suggested a predominance of the alkanes in sedimentary organic matter derived from terrestrial plants. Lignin-derived phenols were generally unrelated to the different ecoregions, perhaps due to the complex composition of deciduous/evergreen trees and the degradation of the phenols in sediments.

References

Abell, J. M., Özkundakci, D., & Hamilton, D. P. (2010). Nitrogen and Phosphorus Limitation of Phytoplankton Growth in New Zealand Lakes: Implications for Eutrophication Control. *Ecosystems*, *13*(7), 966–977. https://doi.org/10.1007/S10021-010-9367-9/FIGURES/3

ACIA. (2005). *Arctic Climate Impact Assessment - ACIA*. http://www.acia.uaf.edu

Adhikari, D. P., & Kumon, F. (2001). Climatic changes during the past 1300 years as deduced from the sediments of Lake Nakatsuna, Central Japan. *Limnology*, *2*(3), 157–168. https://doi.org/10.1007/S10201-001-8031-7/METRICS

Aubry, T. J., Farquharson, J. I., Rowell, C. R., Watt, S. F. L., Pinel, V., Beckett, F., Fasullo, J., Hopcroft, P. O., Pyle, D. M., Schmidt, A., & Sykes, J. S. (2022). Impact of climate change on volcanic processes: current understanding and future challenges. *Bulletin of Volcanology 2022 84:6*, *84*(6), 1–11. https://doi.org/10.1007/S00445-022-01562-8

Bharti, R. R., Adhikari, B. S., & Rawat, G. S. (2012). Assessing vegetation changes in timberline ecotone of Nanda Devi National Park, Uttarakhand. *International Journal of Applied Earth Observation and Geoinformation*, *18*(1), 472–479. https://doi.org/10.1016/J.JAG.2011.09.018

Bianchi, G. G., & McCave, I. N. (1999). Holocene periodicity in North Atlantic climate and deep-ocean flow south of Iceland. *Nature 1999 397:6719*, *397*(6719), 515–517. https://doi.org/10.1038/17362

Bliedtner, M., Schäfer, I. K., Zech, R., & Von Suchodoletz, H. (2018). Leaf wax n-alkanes in modern plants and topsoils from eastern Georgia (Caucasus) - Implications for reconstructing regional paleovegetation. *Biogeosciences*, *15*(12), 3927–3936. https://doi.org/10.5194/BG-15-3927-2018

Bouterfas, R., Belkoura, M., & Dauta, A. (2002). Light and temperature effects on the growth rate of three freshwater algae isolated from a eutrophic lake. *Hydrobiologia*, *489*(1), 207–217. https://doi.org/10.1023/A:1023241006464/METRICS

Brandt, J. P., Flannigan, M. D., Maynard, D. G., Thompson, I. D., & Volney, W. J. A. (2013). An introduction to Canada's boreal zone: ecosystem processes, health, sustainability, and environmental issues. *Environmental Reviews*, *21*(4), 207–226. https://doi.org/10.1139/ER-2013-0040

Bryson, R. A., & Goodman, B. M. (1980). Volcanic Activity and Climatic Changes. *Science*, *207*(4435), 1041–1044. https://doi.org/10.1126/SCIENCE.207.4435.1041

Buchhorn, M., Smets, B., Bertels, L., Roo, B. De, Lesiv, M., Tsendbazar, N.-E., Herold, M., & Fritz, S. (2020). *Copernicus Global Land Service: Land Cover 100m: collection 3: epoch 2019: Globe*. https://doi.org/10.5281/ZENODO.3939050

Canadian Digital Elevation Model, 1945-2011 - Open Government Portal. (n.d.). Retrieved August 6, 2023, from https://open.canada.ca/data/en/dataset/7f245e4d-76c2-4caa-951a-45d1d2051333

Carlson, R. E. (1977). A trophic state index for lakes. *Limnology and Oceanography*,

22(2), 361–369. https://doi.org/10.4319/LO.1977.22.2.0361
Chikaraishi, Y., Naraoka, H., & Poulson, S. R. (2004). Hydrogen and carbon isotopic fractionations of lipid biosynthesis among terrestrial (C3, C4 and CAM) and aquatic plants. *Phytochemistry*, *65*(10), 1369–1381. https://doi.org/10.1016/j.phytochem.2004.03.036
CIFFC | Fire Statistics. (2023). https://ciffc.net/statistics
Collister, J. W., Rieley, G., Stern, B., Eglinton, G., & Fry, B. (1994). Compound-specific δ 13C analyses of leaf lipids from plants with differing carbon dioxide metabolisms. *Organic Geochemistry*, *21*(6–7), 619–627. https://doi.org/10.1016/0146-6380(94)90008-6
Cranwell I, P. A., Eglinton, G., & Robinson, N. (1987). Lipids of aquatic organisms as potential contributors to lacustrine sediments-ll*. *Org. Geochem*, *11*(6), 513–527.
CRANWELL, P. A. (1973). Chain-length distribution of n-alkanes from lake sediments in relation to post-glacial environmental change. *Freshwater Biology*, *3*(3), 259–265. https://doi.org/10.1111/J.1365-2427.1973.TB00921.X
Cronin, T. M., Dwyer, G. S., Kamiya, T., Schwede, S., & Willard, D. A. (2003). Medieval Warm Period, Little Ice Age and 20th century temperature variability from Chesapeake Bay. *Global and Planetary Change*, *36*(1–2), 17–29. https://doi.org/10.1016/S0921-8181(02)00161-3
Cudlín, P., Klopčič, M., Tognetti, R., Mališ, F., Alados, C. L., Bebi, P., Grunewald, K., Zhiyanski, M., Andonowski, V., Porta, N. la, Bratanova-Doncheva, S., Kachaunova, E., Edwards-Jonáová, M., Ninot, J. M., Rigling, A., Hofgaard, A., Hlasny, T., Skalák, P., & Wielgolaski, F. E. (2017). Drivers of treeline shift in different European mountains. *Climate Research*, *73*(1–2), 135–150. https://doi.org/10.3354/CR01465
Duan, Y., Song, J., & Zhang, H. (2004). Carbon isotopic studies of individual lipids in organisms from the Nansha sea area, China. *Science in China, Series D: Earth Sciences*, *47*(7), 593–598. https://doi.org/10.1360/03YD0561/METRICS
Eglinton, G., & Hamilton, R. J. (1967). Leaf Epicuticular Waxes. *New Series*, *156*(3780), 1322–1335.
Eglinton, G., & Logan, G. A. (1991). Molecular preservation. *Philosophical Transactions - Royal Society of London, B*, *333*(1268), 315–328. https://doi.org/10.1098/RSTB.1991.0081
Ertel, J. R., & Hedges, J. I. (1984). *The lignin component of humic substances: Distribution among soil and sedimentary humic, fulvic, and base-insoluble fractions*. *48*.
Ficken, K. J., Li, B., Swain, D. L., & Eglinton, G. (2000). An n-alkane proxy for the sedimentary input of submerged/floating freshwater aquatic macrophytes. *Organic Geochemistry*, *31*(7–8), 745–749. https://doi.org/10.1016/S0146-6380(00)00081-4
Gaire, N. P., Koirala, M., Bhuju, D. R., & Carrer, M. (2017). Site- and species-specific treeline responses to climatic variability in eastern Nepal Himalaya. *Dendrochronologia*, *41*, 44–56. https://doi.org/10.1016/J.DENDRO.2016.03.001
Ganf, G. G., & Oliver, R. L. (1982). Vertical Separation of Light and Available

Nutrients as a Factor Causing Replacement of Green Algae by Blue-Green Algae in the Plankton of a Stratified Lake. *The Journal of Ecology*, *70*(3), 829. https://doi.org/10.2307/2260107

Gehrig-Fasel, J., Guisan, A., & Zimmermann, N. E. (2007). Tree line shifts in the Swiss Alps: Climate change or land abandonment? *Journal of Vegetation Science*, *18*(4), 571–582. https://doi.org/10.1111/J.1654-1103.2007.TB02571.X

Hammer, U. T. (1978). The Saline Lakes of Saskatchewan III. Chemical Characterization. *Internationale Revue Der Gesamten Hydrobiologie Und Hydrographie*, *63*(3), 311–335. https://doi.org/10.1002/IROH.19780630303

Hayes, J. M. (2001). Fractionation of Carbon and Hydrogen Isotopes in Biosynthetic Processes. *Reviews in Mineralogy and Geochemistry*, *43*(1), 225–277. https://doi.org/10.2138/GSRMG.43.1.225

Hedges, J. I., Blanchette, R. A., Weliky, K., & Devol, A. H. (1988). *Effects of fungal degradation on the CuO oxidation products of l&in: A controlled laboratory study*. *52*, 27–44.

Hedges, J. I., & Mann, D. C. (1979a). The characterization of plant tissues by their lignin oxidation products. *Geochimica et Cosmochimica Acta*, *43*(11), 1803–1807. https://doi.org/10.1016/0016-7037(79)90028-0

Hedges, J. I., & Mann, D. C. (1979b). The lignin geochemistry of marine sediments from the southern Washington coast. *Geochimica et Cosmochimica Acta*, *43*(11), 1809–1818. https://doi.org/10.1016/0016-7037(79)90029-2

Herbarium, S. (2008). *Virtual Herbarium of Plants at Risk in Saskatchewan: A Natural Heritage*.

Iiyama, K., Bach, T., Lam, T., & Stonet, B. A. (1990). PHENOLIC ACID BRIDGES BETWEEN POLYSACCHARIDES AND LIGNIN IN WHEAT INTERNODES. *Phytochemistry*, *29*(3), 733–737.

Keatley, B. E., Bennett, E. M., MacDonald, G. K., Taranu, Z. E., & Gregory-Eaves, I. (2011). Land-Use Legacies Are Important Determinants of Lake Eutrophication in the Anthropocene. *PLOS ONE*, *6*(1), e15913. https://doi.org/10.1371/JOURNAL.PONE.0015913

Körner, C., & Paulsen, J. (2004). A world-wide study of high altitude treeline temperatures. *Journal of Biogeography*, *31*(5), 713–732. https://doi.org/10.1111/J.1365-2699.2003.01043.X

Lam, T. B. T., Kadoya, K., & Iiyama, K. (2001). Bonding of hydroxycinnamic acids to lignin: ferulic and p-coumaric acids are predominantly linked at the benzyl position of lignin, not the β-position, in grass cell walls. *Phytochemistry*, *57*(6), 987–992. https://doi.org/10.1016/S0031-9422(01)00052-8

Lamb, H. H. (1965). The early medieval warm epoch and its sequel. *Palaeogeography, Palaeoclimatology, Palaeoecology*, *1*(C), 13–37. https://doi.org/10.1016/0031-0182(65)90004-0

Lécuyer, C., Goedert, J., Klee, J., Clauzel, T., Richardin, P., Fourel, F., Delgado-Darias, T., Alberto-Barroso, V., Velasco-Vázquez, J., Betancort, J. F., Amiot, R., Maréchal, C., & Flandrois, J. P. (2021). Climatic change and diet of the pre-Hispanic population of Gran Canaria (Canary Archipelago, Spain) during the

Medieval Warm Period and Little Ice Age. *Journal of Archaeological Science*, *128*. https://doi.org/10.1016/J.JAS.2021.105336

Leemans, R., & Eickhout, B. (2004). Another reason for concern: regional and global impacts on ecosystems for different levels of climate change. *Global Environmental Change*, *14*(3), 219–228. https://doi.org/10.1016/J.GLOENVCHA.2004.04.009

Liu, G., Sun, L. N., Xu, H., Li, J. H., Li, Z. P., & Li, L. W. (2016). Molecular and carbon isotopic compositions of n-alkanoic acids in smoke from maize straw combustion. *Huanjing Kexue/Environmental Science*, *37*(11), 4156–4161. https://doi.org/10.13227/j.hjkx.201603194

Lockheart, M. J., van Bergen, P. F., & Evershed, R. P. (1997). Variations in the stable carbon isotope compositions of individual lipids from the leaves of modern angiosperms: implications for the study of higher land plant-derived sedimentary organic matter. *Organic Geochemistry*, *26*(1–2), 137–153. https://doi.org/10.1016/S0146-6380(96)00135-0

Lüthi, D., le Floch, M., Bereiter, B., Blunier, T., Barnola, J. M., Siegenthaler, U., Raynaud, D., Jouzel, J., Fischer, H., Kawamura, K., & Stocker, T. F. (2008). High-resolution carbon dioxide concentration record 650,000–800,000 years before present. *Nature 2008 453:7193*, *453*(7193), 379–382. https://doi.org/10.1038/nature06949

MacDonald, G. M. (2010). Some Holocene palaeoclimatic and palaeoenvironmental perspectives on Arctic/Subarctic climate warming and the IPCC 4th Assessment Report. *Journal of Quaternary Science*, *25*(1), 39–47. https://doi.org/10.1002/JQS.1307

Man, M., Pierson, D., Chiu, R., Tabatabaei Anaraki, M., vandenEnden, L., Ye, R. X., Lajtha, K., & Simpson, M. J. (2022). Twenty years of litter manipulation reveals that above-ground litter quantity and quality controls soil organic matter molecular composition. *Biogeochemistry*, *159*(3), 393–411. https://doi.org/10.1007/S10533-022-00934-8/METRICS

Marzi, R., Torkelson, B. E., & Olson, R. K. (1993). A revised carbon preference index. *Organic Geochemistry*, *20*(8), 1303–1306. https://doi.org/10.1016/0146-6380(93)90016-5

Masson-Delmotte, V., Zhai, P., Chen, Y., Goldfarb, L., Gomis, M. I., Matthews, J. B. R., Berger, S., Huang, M., Yelekçi, O., Yu, R., Zhou, B., Lonnoy, E., Maycock, T. K., Waterfield, T., Leitzell, K., & Caud, N. (2021). *Working Group I Contribution to the Sixth Assessment Report of the Intergovernmental Panel on Climate Change Edited by*. www.ipcc.ch

McKenna, J. H., & Doering, P. H. (1995). Measurement of dissolved organic carbon by wet chemical oxidation with persulfate: influence of chloride concentration and reagent volume. *Marine Chemistry*, *48*(2), 109–114. https://doi.org/10.1016/0304-4203(94)00049-J

Meyers, P. A. (1997). Organic geochemical proxies of paleoceanographic, paleolimnologic, and paleoclimatic processes. *Organic Geochemistry*, *27*(5–6), 213–250. https://doi.org/10.1016/S0146-6380(97)00049-1

Meyers, P. A. (2003). Applications of organic geochemistry to paleolimnological reconstructions: a summary of examples from the Laurentian Great Lakes. *Organic Geochemistry*, *34*(2), 261–289. https://doi.org/10.1016/S0146-6380(02)00168-7

Mishra, N. B., & Mainali, K. P. (2017). Greening and browning of the Himalaya: Spatial patterns and the role of climatic change and human drivers. *The Science of the Total Environment*, *587–588*, 326–339. https://doi.org/10.1016/J.SCITOTENV.2017.02.156

Naccarella, A., Morgan, J. W., Cutler, S. C., & Venn, S. E. (2020). Alpine treeline ecotone stasis in the face of recent climate change and disturbance by fire. *PLOS ONE*, *15*(4), e0231339. https://doi.org/10.1371/JOURNAL.PONE.0231339

Nusch, E. A. (1980). Comparison of Different Methods for Chlorophyll and Phaeopigment Determination. *Archiv FUr Hydrobiologie*, *14*, 14–36.

O'Leary, M. H. (1988). Carbon Isotopes in PhotosynthesisFractionation techniques may reveal new aspects of carbon dynamics in plants. *BioScience*, *38*(5), 328–336. https://doi.org/10.2307/1310735

Otto, A., Shunthirasingham, C., & Simpson, M. J. (2005). A comparison of plant and microbial biomarkers in grassland soils from the Prairie Ecozone of Canada. *Organic Geochemistry*, *36*(3), 425–448. https://doi.org/10.1016/J.ORGGEOCHEM.2004.09.008

Otto, A., Simoneit, B. R. T., & Rember, W. C. (2005). Conifer and angiosperm biomarkers in clay sediments and fossil plants from the Miocene Clarkia Formation, Idaho, USA. *Organic Geochemistry*, *36*(6), 907–922. https://doi.org/10.1016/J.ORGGEOCHEM.2004.12.004

Otto, A., & Simpson, M. J. (2006). Evaluation of CuO oxidation parameters for determining the source and stage of lignin degradation in soil. *Biogeochemistry*, *80*(2), 121–142. https://doi.org/10.1007/S10533-006-9014-X/METRICS

Parker, E. N. (1999). Sunny side of global warming. *Nature 1999 399:6735*, *399*(6735), 416–417. https://doi.org/10.1038/20816

Patalano, R., Zech, J., & Roberts, P. (2020). Leaf Wax Lipid Extraction for Archaeological Applications. *Current Protocols in Plant Biology*, *5*(3), e20114. https://doi.org/10.1002/CPPB.20114

Patton, C. J., & Kryskalla, J. R. (2003). Methods of analysis by the U.S. Geological Survey National Water Quality Laboratory-Evaluation of alkaline persulfate digestion as an alternative to Kjeldahl digestion for determination of total and dissolved nitrogen and phosphorus in water. *Water-Resources Investigations Report*. https://doi.org/10.3133/WRI034174

Post-Beittenmiller, D. (2003). BIOCHEMISTRY AND MOLECULAR BIOLOGY OF WAX PRODUCTION IN PLANTS. *Http://Dx.Doi.Org/10.1146/Annurev.Arplant.47.1.405*, *47*(1), 405–430. https://doi.org/10.1146/ANNUREV.ARPLANT.47.1.405

Prabinarana, Dinesh Bhuju, Madan Koirala, & Chuenchit Boonchird. (2017). *Dendroecological studies of rhododendron campanulatum d.Don along the elevational gradient of manaslu conservation area, Nepal Himalaya* [Pakistan

Journal of Botany]. https://www.researchgate.net/publication/320457659_Dendroecological_studies_of_rhododendron_campanulatum_dDon_along_the_elevational_gradient_of_manaslu_conservation_area_Nepal_Himalaya

Redfield, A. C., Ketchum, B. H., & Richards, F. A. (1963). The influence of organisms on the composition of sea-water. *The Sea: Ideas and Observations on Progress in the Study of the Seas*, *2*, 26–77.

Rieley, G., Collister, J. W., Stern, B., & Eglinton, G. (1993). Gas chromatography/isotope ratio mass spectrometry of leaf wax n-alkalines from plants of differing carbon dioxide metabolisms. *Rapid Communications in Mass Spectrometry*, *7*(6), 488–491. https://doi.org/10.1002/RCM.1290070617

Riser, P. G. (1990). The ecological importance of land-water ecotones. In R. J. Naiman & H. Décamps (Eds.), *The Ecology and Management of Aquatic-terrestrial Ecotones* (pp. 7–23). Taylor & Francis. https://books.google.ca/books?id=jFmfXAD7il0C&pg=PA7&lr=&hl=zh-CN&source=gbs_toc_r&cad=4#v=onepage&q&f=false

Sachse, D., Gleixner, G., Wilkes, H., & Kahmen, A. (2010). Leaf wax n-alkane δD values of field-grown barley reflect leaf water δD values at the time of leaf formation. *Geochimica et Cosmochimica Acta*, *74*(23), 6741–6750. https://doi.org/10.1016/J.GCA.2010.08.033

Sachse, D., Kahmen, A., & Gleixner, G. (2009). Significant seasonal variation in the hydrogen isotopic composition of leaf-wax lipids for two deciduous tree ecosystems (Fagus sylvativa and Acerpseudoplatanus). *Organic Geochemistry*, *40*(6), 732–742. https://doi.org/10.1016/J.ORGGEOCHEM.2009.02.008

Saleem, A., Bell, M. A., Kimpe, L. E., Korosi, J. B., Arnason, J. T., & Blais, J. M. (2019). Identifying novel treeline biomarkers in lake sediments using an untargeted screening approach. *Science of The Total Environment*, *694*, 133684. https://doi.org/10.1016/J.SCITOTENV.2019.133684

Schefuß, E., Ratmeyer, V., Stuut, J. B. W., Jansen, J. H. F., & Sinninghe Damsté, J. S. (2003). Carbon isotope analyses of n-alkanes in dust from the lower atmosphere over the central eastern Atlantic. *Geochimica et Cosmochimica Acta*, *67*(10), 1757–1767. https://doi.org/10.1016/S0016-7037(02)01414-X

Schwark, L., Zink, K., Lechterbeck, J., Schwark, L., Zink, K., & Lechterbeck, J. (2002). Reconstruction of postglacial to early Holocene vegetation history in terrestrial Central Europe via cuticular lipid biomarkers and pollen records from lake sediments. *Geo*, *30*(5), 463. https://doi.org/10.1130/0091-7613(2002)030

Schweingruber, F. H. (2012). Tree Rings: Basics and Applications of Dendrochronology. In *Springer Science & Business Media*. https://books.google.ca/books?hl=zh-CN&lr=&id=iyGuBgAAQBAJ&oi=fnd&pg=PP12&dq=Schweingruber,+F.H.+(2012).&ots=qO_9QXDc8P&sig=bHQbA_1LAHYD-PtMFwuMlKu36H4#v=onepage&q=Schweingruber%2C%20F.H.%20(2012).&f=false

Seki, O., Nakatsuka, T., Shibata, H., & Kawamura, K. (2010). A compound-specific

n-alkane δ13C and δD approach for assessing source and delivery processes of terrestrial organic matter within a forested watershed in northern Japan. *Geochimica et Cosmochimica Acta*, *74*(2), 599–613. https://doi.org/10.1016/J.GCA.2009.10.025

Shetty, P., Gitau, M. M., & Maróti, G. (2019). Salinity Stress Responses and Adaptation Mechanisms in Eukaryotic Green Microalgae. *Cells*, *8*(12). https://doi.org/10.3390/CELLS8121657

Simoneit, B. R. T., Sheng, G., Chen, X., Fu, J., Zhang, J., & Xu, Y. (1991). Molecular marker study of extractable organic matter in aerosols from urban areas of China. *Atmospheric Environment. Part A. General Topics*, *25*(10), 2111–2129. https://doi.org/10.1016/0960-1686(91)90088-O

State of the Global Climate 2020. (2021).

Struck, J., Bliedtner, M., Strobel, P., Schumacher, J., Bazarradnaa, E., & Zech, R. (2020). Leaf wax n-alkane patterns and compound-specific δ13C of plants and topsoils from semi-arid and arid Mongolia. *Biogeosciences*, *17*(3), 567–580. https://doi.org/10.5194/BG-17-567-2020

Stuart, G., Gries, C., & Hope, D. (2006). The Relationship between Pollen and Extant Vegetation across an Arid Urban Ecosystem and Surrounding Desert in Southwest USA. *Source: Journal of Biogeography*, *33*(4), 573–591.

Thébault, A., Clément, J. C., Ibanez, S., Roy, J., Geremia, R. A., Pérez, C. A., Buttler, A., Estienne, Y., & Lavorel, S. (2014). Nitrogen limitation and microbial diversity at the treeline. *Oikos*, *123*(6), 729–740. https://doi.org/10.1111/J.1600-0706.2013.00860.X

Theurillat, J. P., & Guisan, A. (2001). Potential impact of climate change on vegetation in the European alps: A review. *Climatic Change*, *50*(1–2), 77–109. https://doi.org/10.1023/A:1010632015572/METRICS

Thevenot, M., Dignac, M. F., & Rumpel, C. (2010). Fate of lignins in soils: A review. *Soil Biology and Biochemistry*, *42*(8), 1200–1211. https://doi.org/10.1016/J.SOILBIO.2010.03.017

US Department of Commerce, N. G. M. L. (2022). *Global Monitoring Laboratory - Carbon Cycle Greenhouse Gases*.

Vane, C. H., Drage, T. C., & Snape, C. E. (2003). Biodegradation of Oak (Quercus alba) Wood during Growth of the Shiitake Mushroom (Lentinula edodes): A Molecular Approach. *Journal of Agricultural and Food Chemistry*, *51*(4), 947–956. https://doi.org/10.1021/JF020932H

Viau, A. E., & Gajewski, K. (2009). Reconstructing Millennial-Scale, Regional Paleoclimates of Boreal Canada during the Holocene. *Journal of Climate*, *22*(2), 316–330. https://doi.org/10.1175/2008JCLI2342.1

Weisberg, P., Shandra, O., & Becker, M. (2018). Landscape Influences on Recent Timberline Shifts in the Carpathian Mountains: Abiotic Influences Modulate Effects of Land-Use Change. *Https://Doi.Org/10.1657/1938-4246-45.3.404*, *45*(3), 404–414. https://doi.org/10.1657/1938-4246-45.3.404

Wetzel, R. G. (2001). Limology Lake and River Ecosystems 3rd ed. *Low Temperature Physics*, *Academic P*(California), 17.

Wetzel, R. G., & Likens, G. E. (2000). *Limnological Analyses* (3rd edition). Springer Press.

William F. Ruddiman. (2000). *Earth's Climate: Past and Future*. W. H. Freeman.

Wotton, B. M., Flannigan, M. D., & Marshall, G. A. (2017). Potential climate change impacts on fire intensity and key wildfire suppression thresholds in Canada. *Environmental Research Letters*, *12*(9), 095003. https://doi.org/10.1088/1748-9326/AA7E6E

Yamada, K., Kamite, M., Saito-Kato, M., Okuno, M., Shinozuka, Y., & Yasuda, Y. (2010). Late Holocene monsoonal-climate change inferred from Lakes Ni-no-Megata and San-no-Megata, northeastern Japan. *Quaternary International*, *220*(1–2), 122–132. https://doi.org/10.1016/J.QUAINT.2009.09.006

Zhang, H. C., Yang, M. S., Zhang, W. X., Lei, G. L., Chang, F. Q., Pu, Y., & Fan, H. F. (2008). Molecular fossil and paleovegetation records of paleosol S4 and adjacent loess layers in the Luochuan loess section, NW China. *Science in China, Series D: Earth Sciences*, *51*(3), 321–330. https://doi.org/10.1007/S11430-008-0012-9/METRICS

Appendix A

GC-MSD Control Parameters
C:\MassHunter\GCMS\2\methods\F1-Alkanes_60m.M
Sample Inlet: Gas Chromatograph, 7890B, Agilent Technologies, Santa Clara, California, United States
Detector: Mass Selective Detector, 5977B, Agilent Technologies, Santa Clara, California, United States

GC Information
Run Time: 58.75 min
Post Run Time: 1 min

Oven
Temperature
Initial: 50 °C
Hold Time: 2.5 min
Post Run: 50 °C
Program
#1 Rate: 16 °C/min
#1 Value: 310 °C
#1 Hold Time: 40 min
Equilibration Time: 1.25 min
Max Temperature: 325 °C

ALS (Automated Liquid Sampler)
Front Injector
Syringe Size: 5 µL
Injection Volume: 1 µL
Solvent A Washes (PreInj): 4
Solvent A Volume: 4 µL
Solvent B Washes (PostInj): 4
Solvent B Volume: 4 µL
Sample Pumps: 6

Front Split/Splitless Inlet, Helium
Mode: Pulsed Splitless
Heater: On 290 °C
Pressure: On 20.256 psi
Total Flow: On 9.3624 mL/min
Septum Purge Flow: On 3 mL/min
Septum Purge Flow Mode: Standard
Gas Saver: On 15 After 2 min mL/min
Injection Pulse Pressure: 20 psi Until 0.9 min

Purge Flow to Split Vent: 5 mL/min at 0.95 min
Liner: 5188-5398 (740 µL, Helix double taper, deactivated), Agilent Technologies, Santa Clara, California, United States

Thermal Aux 2 (MSD Transfer Line)
Temperature: 300 °C

Column
Flow: 1.3624 mL/min
Column Information: 19091S-436, Agilent Technologies, Santa Clara, California, United States
HP-5ms
Temperature Range: 0 °C—325 °C (350 °C)
Dimensions: 60 m x 250 µm x 0.25 µm
Column lock: Locked
In: Front SS Inlet He
Out: MSD
(Initial): 50 °C
Pressure: 20.256 psi
Flow: 1.3624 mL/min
Average Velocity: 31.748 cm/sec
Holdup Time: 2.8275 min
Control Mode: Constant Flow

MSD Information
Acquisition Mode : EI-SIM (Electron Impact - Selected Ion Monitoring)
Solvent Delay (minutes): 7
Tune file: C:\MassHunter\GCMS\2\5977\etune310.u
EM Setting mode Gain: 1.000000
Number of SIM Groups: 1
[SIM Parameters]
Group 1 Group ID: Alkanes
Resolution: 0
Group Start Time: 7
Number of Ions: 2
Ions: Mass 85.05, Dwell 20
MS Source: 310 C maximum 310 C
MS Quad: 150 C maximum 200 C

Appendix B

Elemental Analysis and Stable Isotope Analysis
Ján Viezer Laboratory, University of Ottawa, Ottawa, ON, Canada

Methodology:
Elemental analysis is the determination of the elemental composition of organic or inorganic compounds. The Elementar Isotope Cube is used in the Ján Veizer Lab to determine %N, %C, %H, and %S.
In general, 2-200mg of powdered material or liquid is weighed into tin capsules; material with concentrations down to 0.01% can be analysed on the Elemental Cubes due to their large capacity capabilities. Tungstic oxide (WO3) which acts as a combustion catalyst and binder is added to the capsules in the case of resilient solids, such as salts, (inorganic) sulphur-bearing minerals, iron oxides or alkalis before being closed. Capsules with liquid are flushed with UHP helium before being closed. The closed capsules are re-weighed on the microbalance. Calibrated standards are prepared in a range of weights and run with the samples. A "blind" standard is also run as a check for the calibration.
The prepared capsules are loaded into the carousel of the autosampler. A sample drops down into the top of a column of solid chemicals at 1150°C and is flash combusted at 1800°C for a few seconds with the addition of oxygen. Ultra-pure helium is used to carry the resulting gases through the column of chemicals to finally obtain N2, CO2, H2O, and SO2, then through a series of adsorption traps to separate the gases: using a "trap and purge" method. The thermal conductivity detector (TCD) measures the gases as they are released. Elementar's own software that controls the EA in stand-alone mode is used to process the results from the TCD using various calibration curves, usually linear regression.
The analytical precision (2 sigma) for the analyses is +/- 0.2%.

Instrumentation:
NC: model Vario EL Cube, Elementar, Germany
NCS, NCHS, Special N, S configurations: model Vario Isotope Cube, Elementar, Germany

Supplementary Data

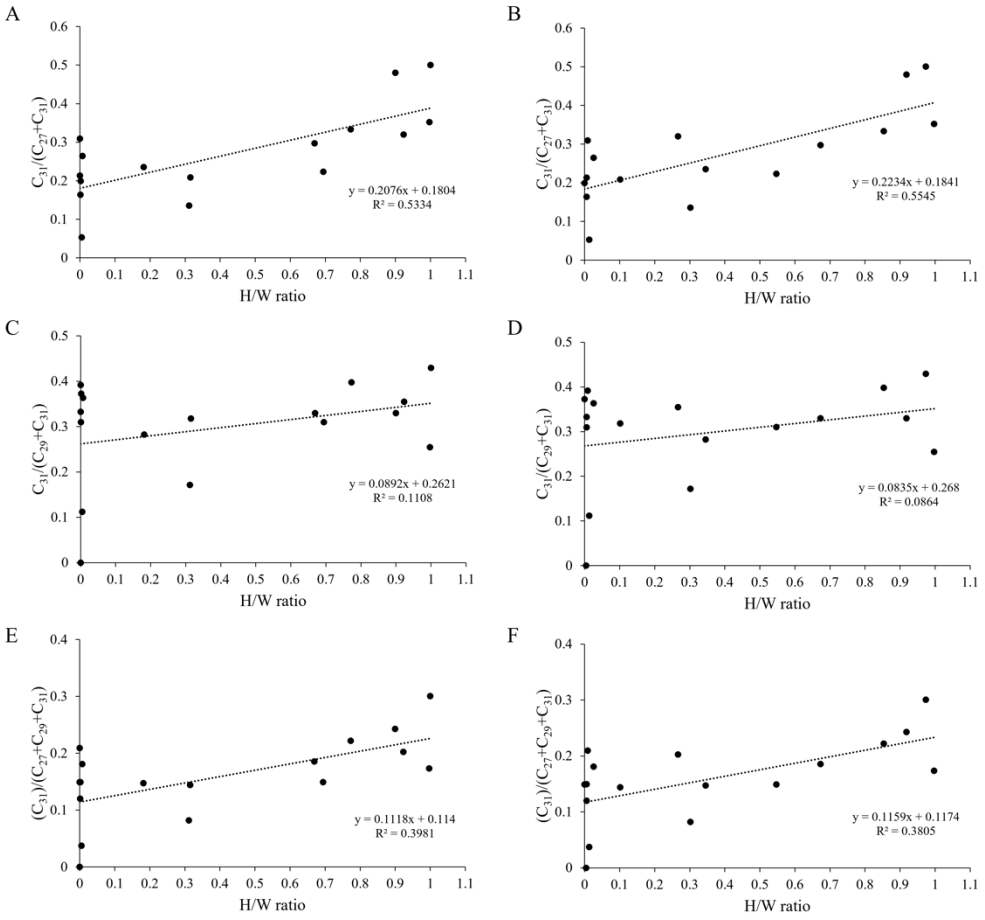

Fig. S1. Linear regression between Herbaceous to Woody plants relative ratio (H/W ratio) and $C_{31}/(C_{27}+C_{31})$, $C_{31}/(C_{29}+C_{31})$, and $C_{31}/(C_{27}+C_{29}+C_{31})$ for Accumulation maps (A, C, E) Buffer maps (B, D, F).

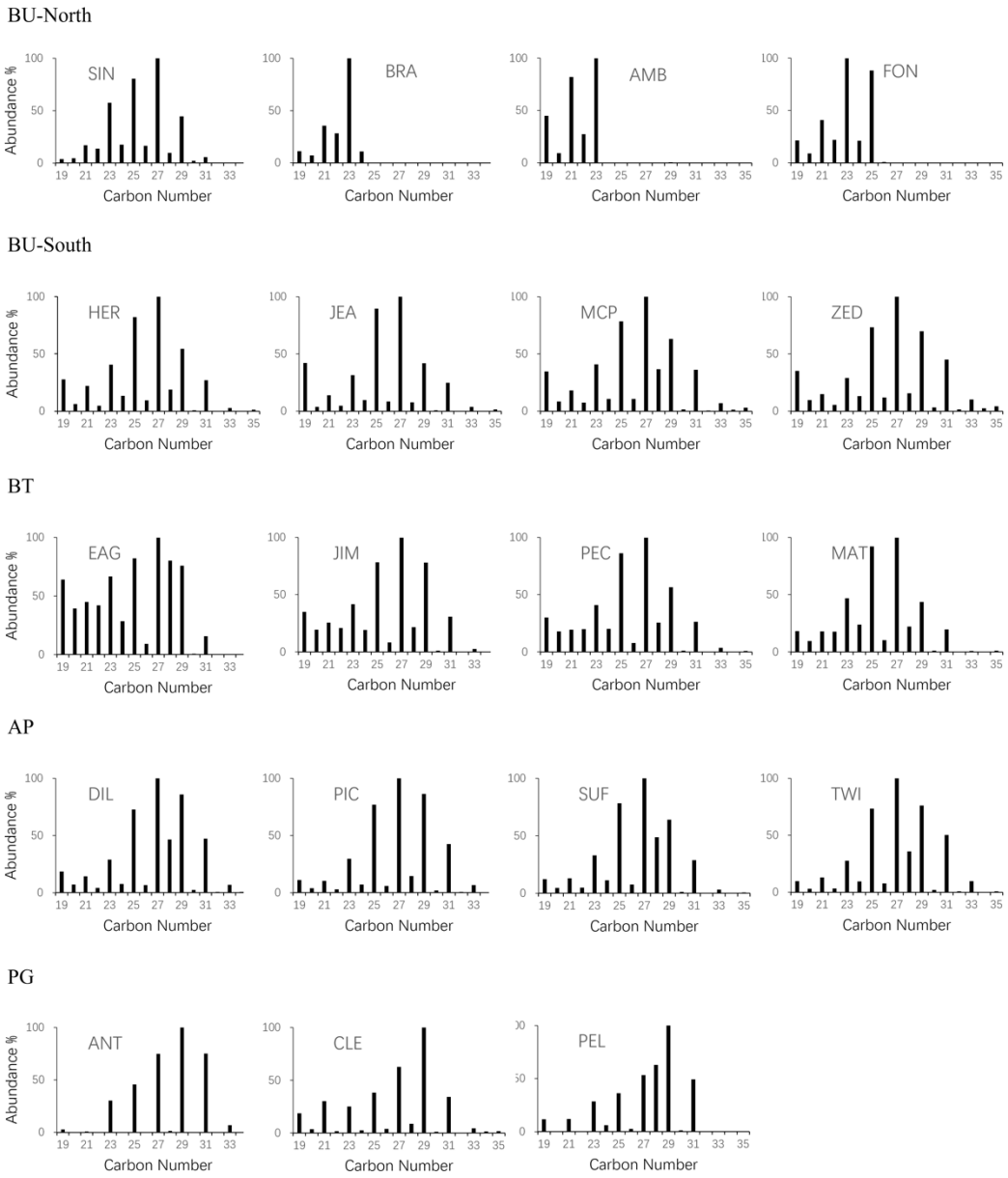

Fig. S2. Histograms of *n*-alkane abundance relative to the C_{max} in the Saskatchewan lake sediments.